ELSEVIER

Chemical Geology 226 (2006) 79–99

CHEMICAL GEOLOGY
INCLUDING
ISOTOPE GEOSCIENCE

www.elsevier.com/locate/chemgeo

A chemical Earth model with whole mantle convection: The importance of a core–mantle boundary layer (D″) and its early formation

I.N. Tolstikhin [a], J.D. Kramers [b,*], A.W. Hofmann [c]

[a] *Geological Institute, Kola Scientific Centre of Russian Academy of Sciences, 184200 Apatity, Russia*
[b] *Laboratory of Isotope Geology, Institute of Geological Sciences, University of Bern, Erlachstrasse 9a, Bern 3012 Switzerland*
[c] *Max Plank Institute fur Chemie, Abt. Geochemie, Joh.-J.-Becher-Weg 27 D 55128 Mainz, Germany*

Accepted 5 September 2005

Abstract

Advances in seismic tomography and mantle convection modeling have led to the convincing conclusion of whole-mantle convective flow, so that compositional differences between upper and lower mantle could not have been preserved over the age of the earth. Nevertheless, there is compelling geochemical evidence favoring the occurrence of an ancient apparently isolated reservoir. We propose this reservoir is located in the core–mantle transition (termed D″). It was formed during the late stages of Earth accretion via subduction of primitive mafic to ultramafic crust along with a terrestrial regolith composed (partially) of chondritic and solar–wind-implanted material. To investigate this scenario we develop a quantitative geochemical model envisaging accretion of the Earth from chondrite-like material, formation and evolution of the principal terrestrial reservoirs (the mantle, core, D″, continental crust) via mass fluxes that include rare gas and respective parent isotopes, also Sm, Nd, Lu, Hf, Rb, Sr, W isotopes and siderophile elements. The solution shows that such a model, with a D″ mass of $\sim 2\times 10^{26}$ g and a regolith proportion of ~ 1/4, allows the apparent conflict between geophysical and geochemical observations to be resolved.

Keywords: Mantle; Crust; Isotopic systematics; Trace elements; Siderophile elements; Modeling

1. Introduction

The advances in high-resolution seismic tomography and mantle convection modeling have led to the conclusion that convective flow encompasses the whole mantle and thus this reservoir is efficiently mixed (Grand, 1994; Christensen, 1995; van der Hilst et al., 1997; Puster and Jordan, 1997; Bunge et al., 1998; van Keken and Zhong, 1999; Montelli et al., 2004). This means that large-scale mantle heterogeneities especially those formed early in Earth history are unlikely to have been preserved (van Keken et al., 2002). Much more vigorous convection is furthermore expected in early Earth evolution, at least during the first ~500 Ma after Earth accretion, and this further reinforces the above conclusion (Tolstikhin and Marty, 1998, see Section 7.2).

Geochemical data discussed briefly in Section 2 are in apparent conflict with this outcome of geophysical observations and models. In an attempt to outline a unified Earth model capable of resolving this conflict, it has been proposed that a small core-mantle transition zone (formed during late stages of Earth accretion from

* Corresponding author. Fax: +41 31 631 4988.
E-mail address: kramers@geo.unibe.ch (J.D. Kramers).

0009-2541/$ - see front matter © 2005 Elsevier B.V. All rights reserved.
doi:10.1016/j.chemgeo.2005.09.015

subducted basaltic crust along with terrestrial chondrite-like regolith) could be a geochemically important reservoir (Tolstikhin and Hofmann, 2005). In this contribution we develop a simple transport balance model and apply it to the proposed scenario. Even though such models do not generate a unique solution, they can illustrate whether a solution is plausible, which parameters are important, and constrain poorly known or unknown parameters.

Our modeling strategy is based on distinct reservoirs. Here we differ from Meibom and Anderson (2003) who support the view "that statistical distributions of lithologic components and sampling theory should replace the concept of distinct isolated geochemical reservoirs, and extensive convective stirring prior to sampling". Rather, two approaches are possible. One is the investigation, generally performed within the frame of a steady state approximation, of the fine structure of a reservoir, sources and scales of its heterogeneities and reasons why these heterogeneities are preserved. Another is the study of when and how a given reservoir could have been formed and developed. Here the average compositions of reservoirs can be used.

Three types of chemical evolutionary models may be distinguished (in order of increasing complexity): (1) transport models envisaging distinct homogeneous reservoirs and applying mainly mass balance considerations (e.g., O'Nions et al., 1979; Jacobsen and Wasserburg, 1979); (2) transport chemical models envisaging the temporal preservation of chemical and isotopic heterogeneities, which highlight the behaviour of species within each reservoir considered (Kellogg et al., 2002); (3) physical models with chemical tracers in them (Christensen and Hofmann, 1994; van Keken et al., 2002; Samuel and Farnetani, 2003).

Such models are best applied progressively, increasing complexity only when simpler approaches and their deficiencies are understood. In this contribution we aim to make a start by applying a simple transport model to multiple isotope and trace element systems in order to study an initially chondritic whole-mantle-convective Earth. The model includes two major stages of Earth history, accretion and post-accretion evolution. The relevant geochemical and isotopic systems are: ^{182}Hf–^{182}W, refractory moderately and highly siderophile elements, ^{244}Pu–Xe(Pu), ^{129}I–^{129}Xe(I), ^{40}K–^{40}Ar, U–Th–He(Ne), ^{147}Sm–^{143}Nd, ^{176}Lu–^{176}Hf, and ^{87}Rb–^{87}Sr.

Only one reference solution of the model is presented. The importance of the parameters and how their variations influence the solution are to be discussed in later contributions. Problems related to the composition and evolution of the terrestrial atmosphere are marginally relevant in this contribution, and we refer to observed atmospheric abundances of species of interest only where these are important for the balance in the solid earth.

2. Geochemical indicators for the occurrence of an early-formed, apparently isolated reservoir

There is diverse geochemical evidence for an ancient apparently isolated reservoir. Most of this evidence has been widely discussed in the literature and we only briefly review it here. The isotopic signatures of rare gases in the mantle are especially important and convincing: rare gas abundances in meteoritic and potential prototerrestrial materials are many orders of magnitude below the solar abundance (a direct consequence of rare gas "nobility"). Therefore noble gas isotopic anomalies are readily seen above the terrestrial background.

2.1. Paradox of radiogenic xenon isotopes

Xe includes a radiogenic isotope, ^{129}Xe, resulting from the decay of extinct ^{129}I (half-life 15.7 Ma) and fissiogenic isotopes, particularly ^{136}Xe, resulting from fission of ^{238}U (4.47 Ga) and extinct ^{244}Pu (80 Ma). The original abundances of the extinct parent isotopes in the Earth can be estimated with reasonable confidence (see Table 1) and would result in a ^{129}Xe(I)/^{136}Xe(U) ratio of ~3000 and a ^{136}Xe(Pu)/^{136}Xe(U) ratio of ~40 if no loss of Xe had occurred at all. However, the ratios observed in mantle Xe are ^{129}Xe(I)/^{136}Xe(U) ≈ 3 and ^{136}Xe(Pu)/^{136}Xe(U) <0.4, lower than the closed system values by factors of 1000 and >100, respectively. A first conclusion is that loss of both ^{129}Xe(I) and ^{136}Xe(Pu) has occurred early in Earth history. Further, if the solid Earth is modeled as a single reservoir, a paradox arises: Fitting the observed value for ^{129}Xe(I)/^{136}Xe(U) requires a much shorter degassing time scale than that needed for reconciling ^{136}Xe(Pu)/^{136}Xe(U) (see Kunz et al., 1998).

A present-day ratio of ^{129}Xe(I)/^{136}Xe(U) ≈ 3, similar to that observed, results from a model in which it is assumed that Xe was almost completely lost up to about 4.47 Ga ago and that no significant further loss occurred subsequently. The short-lived parent isotope ^{129}I would have been almost completely decayed by the time its daughter isotope ^{129}Xe(I) was lost, while ^{136}Xe(U) would continue to be produced by fission of long-lived ^{238}U. Only a small portion of ^{136}Xe(U) was generated and lost before 4.47 Ga ago, so that the

early Xe loss did not substantially affect the amount of $^{136}Xe(U)$ in the reservoir.

However, this model of closure at 4.47 Ga yields a $^{136}Xe(Pu)/^{136}Xe(U)$ ratio about 50 times larger than observed. In order to obtain a good fit for $^{136}Xe(Pu)/^{136}Xe(U)$, a much later closure of the system, at ~4 Ga, must be invoked. By this time ~99% of ^{244}Pu would have been decayed, and the remaining 1% would subsequently have produced the observed $^{136}Xe(Pu)/^{136}Xe(U)$ ratio. Needless to say, no measurable $^{129}Xe(I)$ would now have been present on Earth with such a late closure time.

The traditional explanation, or solution, of this mantle xenon paradox (since the early inspiring paper by Butler et al., 1963) makes use of two reservoirs: (1) an ancient reservoir, which became isolated very early in

Table 1
Input parameters: mass and composition of prototerrestrial materials and respective decay constants

Parameter	Dimensions	Value	Notes
Mass of reservoir	Gram	5.98×10^{27}	1
Metal/total mass ratio	Ratio	0.3275	1
Chondrite/basalt ratio	Ratio	0.2	1
^{232}Th	Atoms/g	1.57×10^{14}	2
$^{232}Th/^{238}U$	Atomic	2.41	2
$^{235}U/^{238}U$		0.316	
$^{244}Pu/^{238}U$	Atomic	0.01	3
$^{127}I/^{232}Th$	Atomic	0.206	4
$^{129}I/^{127}I$		0.0001	5
$^{40}K/^{238}U$	Atomic	52	6
^{144}Nd		8.40E+14	7
$^{143}Nd/^{144}Nd$		0.506673	8
$^{147}Sm/^{144}Nd$	Atomic	0.202665	8
$^{144}Nd/Nd$	Atomic	0.23794	8
^{177}Hf	Atom/g	1.21×10^{14}	9
$^{176}Hf/^{177}Hf$		0.27982	10
$^{176}Lu/^{177}Hf$	Atomic	0.03615	10
$^{177}Hf/Hf$	Atomic	0.18599	10
^{86}Sr	Atoms/g	9.15×10^{15}	11
$^{87}Sr/^{86}Sr$		0.69876	12
$^{87}Rb/^{86}Sr$	Atomic	0.0864	13
Co, Ni, Mo, Ir, Re, Au	Norm. ratio	0.6725	14
^{184}W	Norm. ratio	0.6725	15
$^{182}W/^{184}W$		0.8643	16
$^{180}Hf/^{184}W$	Atomic	1.33	16
$^{182}Hf/^{180}Hf$		0.00014	16
$^{4}He/^{3}He_{SIN}$		2310	17
$^{36}Ar/^{3}He_{SIN}$		0.066	18
$^{40}Ar/^{36}Ar_{SIN}$		0.01	18
$^{130}Xe/^{3}He_{SIN}$		1.6E-07	18
$^{3}He/^{130}Xe_{Q}$		0.323	19
$^{4}He/^{130}Xe_{Q}$		2300	19
$^{36}Ar/^{130}Xe_{Q}$		470	19
$^{40}Ar/^{130}Xe_{Q}$		4.7	19
$^{129}Xe/^{130}Xe_{Q}$		6.31	19
$^{136}Xe/^{130}Xe_{Q}$		1.95	19
λ_{244}	Ga^{-1}	8.41	20
λ_{238}	Ga^{-1}	0.155125	
λ_{235}	Ga^{-1}	0.98485	
λ_{232}	Ga^{-1}	0.049475	
λ_{182}	Ga^{-1}	77.01635	
λ_{176}	Ga^{-1}	0.01865	
λ_{147}	Ga^{-1}	0.00654	
λ_{129}	Ga^{-1}	44.15	
λ_{87}	Ga^{-1}	0.01402	
λ_{40}	Ga^{-1}	0.5543	

Notes to Table 1:
(1) First two rows: same as for the present-day Earth; third row: this proportion of chondrite-like material is enough to increase the mean basalt+regolith density by 7% and to stabilize this mixed material at the bottom of the convective mantle (Kellogg, 1997).
(2) Corresponds to U=19 ppb and Th/U=3.9 in the present-day BSE (Rocholl and Jochum, 1993).
(3) Meteoritic mean (see compilation by Azbel and Tolstikhin, 1993). This is close to the upper limit of the canonical ratio $^{244}Pu/^{238}U_{INI}=0.0068\pm0.003$ (Hudson et al., 1982).
(4) Corresponds to 10 ppm of ^{127}I in the BSE (Deruelle et al., 1992; Muramatsu et al., 2001; Muramatsu and Wedepohl, 1998).
(5) Meteoritic mean (e.g., Swindle and Podosek, 1988).
(6) Corresponds to the present-day mass ratio $K/U_{BSE}=12{,}000$ (Jochum et al., 1983).
(7) Corresponds to 1250 ppb of Nd in BSE (McDonough and Sun, 1995).
(8) Chondritic systematics (Jacobsen and Wasserburg, 1980a; Jacobsen et al., 1984; Wasserburg et al., 1981).
(9) From McDonough and Sun (1995).
(10) After Blichert-Toft and Albarède (1997).
(11) After McDonough and Sun (1995).
(12) After Wasserburg et al. (1977).
(12, 13) After Hofmann (1988) and McDonough and Sun (1995); corresponds to present-day K/Rb=400 and $^{87}Sr/^{86}Sr_{BSE}=0.7041$. The latter is slightly below the value of 0.7045 (Jacobsen and Wasserburg, 1979), which is widely used but not really constrained (Blichert-Toft and Albarède, 1997).
(14) Chondritic abundances normalized to C1 and Al that give ≡1 in the mantle if siderophile elements would not have been sequestered into the core.
(15) In the case of tungsten, ^{184}W stands instead of element because it is the reference isotope for ^{182}Hf–^{182}W systematics.
(16) Similar to Kleine et al. (2002), Schoenberg et al. (2002), Yin et al. (2002).
(17, 18) The solar implanted nuclide (SIN) abundances could be different from solar wind (SW) and/or solar energetic particles (SEP) because of much more intense solar radiation during the first ~100 Myr after solar system (SOS) formation (see Wood et al., 2002). Also the astrophysical environment in which the implantation occurred is unknown. To highlight this possible difference we have used another abbreviation. The value listed for note 17 is after Pedroni and Begemann (1994), values for note 18 are assumed to be similar to the implanted solar wind (Anders and Grevesse, 1989). The isotope composition of Xe_{SIN} is not important because Xe_Q is by far the major Xe component (see Section 5).
(19) After Busemann et al. (2000).
(20) Decay constants and $^{40}K\rightarrow{}^{40}Ar$ branching ratio 0.1048 (after Villa and Renne, 1998). The fission branching ratios and ^{136}Xe yields are 5.45×10^{-7} and 0.063 for ^{238}U and 0.00125 and 0.056 for ^{244}Pu, respectively (Ozima and Podosek, 2002).

Earth history, and contains most of terrestrial $^{129}Xe(I)$, and (2) the convecting, continuously degassed mantle, which communicates with the atmosphere through volcanism and subduction. The first reservoir is envisaged to be incompletely closed, and the observed $^{129}Xe(I)/^{136}Xe(U)$ ratio would result from "leakage" of $^{129}Xe(I)$ into the second reservoir. In principle a single-reservoir degassing model can also be reconciled with the observed abundances of mantle and atmospheric xenon (to be published elsewhere). However, some of the consequences of this model generate new problems. For instance, this model would require very late loss of xenon from the Earth's atmosphere, at ~3.8 Ga ago, but fingerprints of this dramatic event have not yet been discovered in the geological record and respective geochemical systematics (e.g., K–Ar). Therefore the 2-reservoir-model is still by far the most plausible solution for the mantle xenology paradox.

2.2. Primordial solar He and Ne; heat fluxes

The $^{4}He/^{3}He$ and $^{21}Ne/^{22}Ne$ ratios in some plume-derived rocks and fluids (e.g., Fig. 1 in Tolstikhin and Hofmann, 2005, see also Dixon et al., 2000; Moreira et al., 2001) are much lower than the relatively uniform ratios in mid-ocean ridge basalt (MORB) samples and require low time-integrated (U, Th)/^{3}He and (U, Th)/^{22}Ne ratios in a respective source reservoir. Previously, modeling of light noble gas characteristics of the upper mantle has been based on the concept of influx from a large reservoir, the lower mantle (O'Nions and Oxburgh, 1983: Kellogg and Wasserburg, 1990; Porcelli and Wasserburg, 1995). Further, O'Nions and Oxburgh (1983) pointed out that heat and helium fluxes from the Earth's mantle are "most readily compatible with a convecting upper mantle, which loses its small amount of radiogenic heat and helium efficiently but which is isolated from a lower mantle reservoir" which generates the major portion of the terrestrial radiogenic heat. Recently van Keken et al. (2001) reviewed this problem and confirmed the validity of the above conclusion.

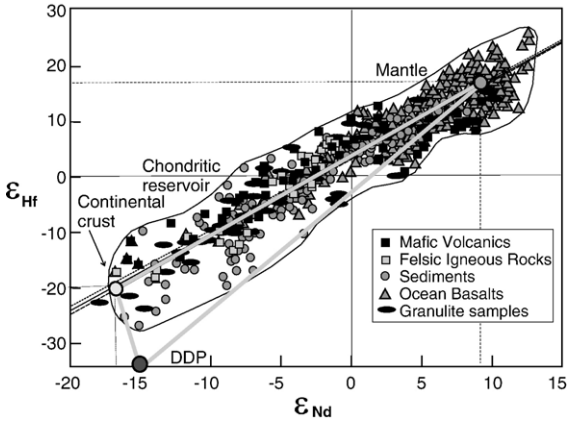

Fig. 1. The terrestrial $\varepsilon(Hf)$ versus $\varepsilon(Nd)$ array (Vervoort et al., 1999, 2000). The three regression lines for the mantle- and crustal-derived sub-sets and for the complete data set are very similar and all pass by about +3 $\varepsilon(Hf)$ units above chondritic $\varepsilon(Nd)$–$\varepsilon(Hf)$ values for the bulk silicate earth. Circles are the average ε values derived from the reference solution of the model for the three reservoirs involved. The model-derived mantle–crust connection (thick gray line) is indistinguishable from the regressions of the data (see references for data-sources in these contributions).

2.3. Lithophile mass balances

The rare earth elements are particularly suitable for addressing problems of the Earth's chemical inventory: They are all involatile and lithophile, so that their initial BSE abundances can be reliably restored from meteoritic data. They are also (in most cases) incompatible, and their behavior in terrestrial fractionation processes is relatively simple and well understood. Further, isotopic systematics are available along with the chemical data. Therefore REEs and especially the ^{147}Sm–^{143}Nd isotope systematics have been widely used to model terrestrial fractionation processes as well as the evolution and present-day structure of the Earth.

The isotopic record of Sm–Nd systematics shows that it is difficult to reconcile the present-day bulk silicate Earth (BSE) inventory of refractory non-siderophile elements with the chondritic initial abundances if the elements are distributed between two complementary reservoirs: the depleted MORB-source mantle (DM) with mass M_{DM} and Nd concentration Nd_{DM}, and the continental crust (CC, M_{CC}, Nd_{CC}). The mass balance (e.g., Allegre, 1997) dictates:

$$M_{CC}Nd_{CC}\varepsilon(Nd)_{CC} + M_{DM}Nd_{DM}\varepsilon(Nd)_{DM} = (M_{CC} + M_{DM})\varepsilon(Nd)_{BSE} \quad (1)$$

where $\varepsilon(Nd) = 10000 \times (({}^{143}Nd/{}^{144}Nd)_{RES}/({}^{143}Nd/{}^{144}Nd)_{BSE} - 1)$ refers to the Nd isotope composition in a given reservoir relative to the bulk silicate earth, which is assumed to be of chondritic composition. Hence $\varepsilon(Nd)_{BSE} \equiv 0$ and

$$M_{DM} = -(M_{CC}Nd_{CC}\varepsilon_{CC}/Nd_{DM}\varepsilon_{DM}). \quad (2)$$

Substituting in (2) $Nd_{DM}=0.9$ ppm (McKenzie and O'Nions, 1991) and $\varepsilon_{DM}=9$ (well defined, Section 6.2) along with the upper limit for $Nd_{CC}=26$ ppm (e.g., Wedepohl, 1995) and lower limit for $\varepsilon_{CC}=-21$ (Fig. 1) gives a maximum depleted mantle mass of ~0.4 × total

mantle. A primitive or enriched reservoir is thus required to store a considerable portion of Nd (as well as all other refractory lithophile trace elements). Early evolutionary models by O'Nions et al. (1979), Jacobsen and Wasserburg (1979, 1980b), DePaolo (1980) and Azbel and Tolstikhin (1988) led to very similar conclusions and corroborated a layered mantle concept.

2.4. Lu–Hf and Sm–Nd misfit

A combined inventory of terrestrial Lu–Hf and Sm–Nd systematics (including mantle and crustal rocks, both magmatic and sedimentary) gives a coherent ε(Hf) versus ε(Nd) array with ε(Hf) data-points lying about +3 ε(Hf) units above the chondritic value, considered to also represent the BSE (Fig. 1). Chase and Patchett (1988) proposed an explanation for this discrepancy: early formed mantle melts were in equilibrium with garnet and therefore left behind a residual mantle with enhanced Lu/Hf ratio; these melts formed an early crust, which was subducted and isolated from the convecting mantle. This scenario, discussed in several later contributions (e.g., Blichert-Toft and Albarède, 1997; Blichert-Toft and Arndt, 1999), reconciles the super-chondritic Hf isotopic composition (as observed in the terrestrial array) and an initially chondritic bulk silicate earth. Recent re-investigation of Lu–Hf isotope systematics in chondritic meteorites by Patchett et al. (2004) has shown that both $^{176}Hf/^{177}Hf$ and $^{176}Lu/^{177}Hf$ ratios vary substantially and therefore it is difficult to constrain the BSE parameters precisely. However, on the whole the meteoritic data still lead to $\varepsilon(Hf)_{BSE}$ somewhat below the terrestrial Hf–Nd array.

To explain these observations several proposals have been put forward. All of these have deficiencies. (i) Most proposals consider only some of the observations (e.g., mantle rare gases, Albarède, 1998; Porcelli and Halliday, 2001; Trieloff and Kunz, 2005; Class and Goldstein, 2005). (ii) Layered-mantle models proposed to account for the geochemical observations invoke large lower mantle reservoirs that have not been observed in seismic tomography (e.g., Kellogg et al., 1999). (iii) It has not been suggested as yet when and how a long-lived distinct mantle reservoir could have been formed and stabilized (e.g., van Keken et al., 2002; Samuel and Farnetani, 2003).

3. The proposal: D″ as an early-formed apparently isolated geochemically important reservoir

Recently Tolstikhin and Hofmann (2002, 2005) proposed that the region at the base of the mantle (termed D″, the abbreviation DDP is used in suffixes) constitutes the largely isolated reservoir containing the missing components of the terrestrial budget. The present mass of this layer, from seismic data, is 2.31×10^{26} g, (see discussion in Tolstikhin and Hofmann, 2002, 2005). A recent exciting discovery by Boyet and Carlson (2005) may lend support to this proposal: They reported $^{142}Nd/^{144}Nd$ analyses on 6 chondritic meteorites and showed these to be consistently below the terrestrial value, with an average offset of −20 ppm. Within the frame of the chondritic Earth model this means that the known silicate Earth as a whole became LREE-depleted when ^{142}Nd (half-life 103 Ma) was still significant. In other words, a LREE-enriched reservoir must have become permanently separated from it. The explanation suggested by Boyet and Carlson (2005) is that relatively LREE-enriched mafic crust, formed by mantle partial melting, was sequestrated in the D″ layer in earliest Earth history.

Tolstikhin and Hofmann (2002, 2005) envisaged that this layer was formed as a result of the loading of an early terrestrial mafic to ultramafic crust with a late accretion "veneer" of average chondritic composition, which made it intrinsically denser than silicate mantle material so that it could sink and reside stably at the base of the mantle. This proposal has a basis in models for the formation of the terrestrial planets that include the effect of Jupiter and Saturn on the asteroid belt (Chambers and Wetherill, 2001; Morbidelli et al., 2000). On the one hand, models predict that collisions with planet-sized bodies (such as gave rise to the Moon) form the dominant contribution to late Earth accretion (Angor et al., 1999). On the other hand, resonances between the giant planets and the asteroid belt would have caused scattering and collisions in this belt, causing most of its mass to be lost from it. If the original eccentricity of the orbits of Jupiter and Saturn was low, this "clearing" could have happened tens of Ma after the start of solar system formation, at a time when the Earth was almost fully accreted (Chambers and Wetherill, 2001). It is reasonable to assume that at this stage small planetesimals, collision-related fragments and dust collided with the Earth (Morbidelli et al., 2000).

Whether material arrived in large or in small impacts greatly affected how it was incorporated in the Earth. The kinetic energy of large impactors was deposited at some depth below the Earth's surface. It caused melting, degassing and even vaporization, vigorous convection and mixing of impactor and target materials (Pierazzo and Melosh, 1999). Then metal/silicate fractionation and metal transfer into the core followed,

leaving behind metal- and siderophile element-free degassed silicate material. The silicate melts formed an early basaltic to komatiitic crust. In contrast, smaller bodies would merely load the crust, contributing to a terrestrial regolith.

The late accreting matter probably would have included differentiated as well as chondrite-like material, and its average composition may have been close to chondritic, with a volatile component retained in part of it. Because the solar nebula was transparent at that time, solar emissions irradiated their surfaces gardened by collisions; therefore the thickness of the solar-gas-rich regolith may have been considerable. As these bodies fell on the Earth and loaded the early crust, the rare-gas-rich material could have survived atmospheric ablation and preserved appreciable amounts of initially trapped Q and implanted solar gases, as demonstrated today by solar-rare-gas-rich meteorites, Q-gas-rich chondrites and meteorites bearing sub-solar rare gases (Poupeau et al., 1974; Busemann et al., 2000, 2003).

The early basaltic/komatiitic crust was probably thicker and denser than present-day oceanic crust, because of the high degree of melting that caused it and owing to its ultramafic component (e.g., Chase and Patchett, 1988). Its bulk density increased further through loading by a (on average) chondrite-like regolith containing metallic iron. This means that, when the crust was subducted, it is likely to have descended to the core mantle boundary, where it formed a semi-permanent dense layer. The intrinsic enrichment in iron and silica would allow this layer to be stabilized, in full accord with recent proposals (Samuel et al., 2003; Mao et al., 2004). There may be other mechanisms for D″ stabilization. These include the formation of a dense post perovskite phase (Oganov and Ono, 2004), or the formation of iron-rich dense silicate melts (Lay et al., 2004). In any case, only material accumulated in D″ after the Moon-forming Giant Impact could have been preserved in this way, as this event almost certainly entailed whole-mantle melting.

This scenario provides a natural explanation of how a "late veneer" could have been transferred from the Earth's surface into the mantle, developing specific noble gas and siderophile element abundance patterns in the deep Earth, and why a repository for at least some of this veneer could have become isolated from the convecting mantle. Small mass (and/or species) fluxes from D″ into the convecting mantle could have subsequently maintained a mantle rare gas isotope signature throughout Earth's history. Naturally, mixing of some of the subducting crust+regolith assemblage with the material of the convecting mantle could have occurred before this assemblage approached the core–mantle boundary, thus ensuring delivery of siderophile elements directly into the mantle.

4. Earth accretion and evolution: the model

We describe the above scenario by a transport model similar to those published previously (Kramers and Tolstikhin, 1997; Kramers, 1998; Tolstikhin and Marty, 1998).

The main stage of Earth accretion is portrayed as a mass flux from a reservoir of prototerrestrial material (ptm, see Table 1 below) into the silicate shell of the earth (bulk mantle, bml, Fig. 2A). The silicate Earth is envisaged as a vigorously convecting reservoir, so that mixing of metal-bearing accreting material with metal-depleted mantle material precedes metal–silicate fractionation. The fractionation occurs in a mantle fractionation zone, mf, melted either as a result of impact, or/and through decompression resulting from convection. Within this zone liquid and solid metal and silicate phases separate from the bulk mixed mantle material. Trace elements are partitioned among these phases, whereby equilibrium partitioning is envisaged (see Eqs. (3), (4) and (6) in Kramers, 1998). The metal/silicate partition coefficients change in the course of the process following a general increase of oxygen fugacity (Righter et al., 1997; Kramers, 1998). Metal is segregated in mf, followed by merging and settling of droplets, and can ultimately form blobs or diapirs large enough to sink though the mantle and join the core (see Eqs. (1) and (2) in Kramers, 1998). The metal fraction of the mantle $F(\mathrm{met})_{\mathrm{bml}}$ is controlled by the feeding flux carrying a constant portion of metal, 0.327, by the mantle mass $M_{\mathrm{bml}}(t)$, and by the mantle–core metal-removing flux. Obviously the metal fraction decreases from the above value at the start of core segregation to very low values during the late stages of the process. Even after accretion has ceased, core growth continues as long as the metal content in the mantle fractionation zone is large enough to allow metal settling. The liquid silicates form a basaltic (komatiitic) crust (boc) and then, along with the solid silicates, return to the mantle and are re-mixed within this reservoir.

During late accretion, part of this early crust is loaded with prototerrestrial material irradiated by solar corpuscular radiation as discussed above. The basaltic crust, along with this "terrestrial regolith", sinks to the core–mantle boundary, and forms the D″' reservoir. A basalt/regolith mass ratio of (4/1) results in a density contrast large enough to stabilize this mix at the core–mantle boundary.

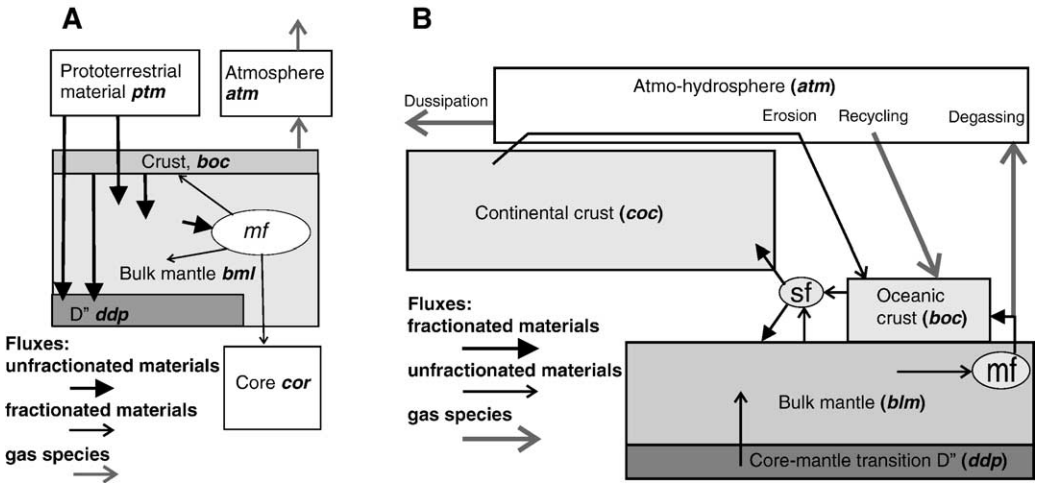

Fig. 2. Schematic presentation of chemical transport model. (A) Accretion-core formation fluxes and processes envisaged by the model. (B) Post-accretion fluxes and processes. Partial melting and fractionation domains are: mf for MORB-production, and sf for continental crust formation (equivalent to mantle wedge above subduction zones).

After accretion and core-segregation have ceased, decompression-related partial melting and fractionation in a mantle fractionation zone continue, producing a flux of liquid silicates that forms a short-lived crust boc (Fig. 2B). The rare gas constituents of this flux are quantitatively released into the atmosphere (atm), which undergoes early gas dissipation processes. The oceanic crust is being contaminated by material eroded from the continents and by atmospheric rare gases (Eqs. (A2.4) and (A2.13) in Tolstikhin and Marty, 1998). The mass of the oceanic crust is small and constant. While new crust is generated via mf-fractionation, an out-flux of an equivalent portion of the contaminated crust is split: the major part returns to the mantle, whereas the minor part enters the subduction-related fractionation zone sf; the proportion of splitting is governed by the continental-crust-generating flux of liquid silicate (see Eq. (9) in Kramers and Tolstikhin, 1997).

The model envisages the subduction-related fractionation sf as the only process supplying the continental crust (coc) with mass and species (Fig. 2B). To model crustal growth, Jacobsen (1988) and Azbel and Tolstikhin (1988) introduced the age distribution function $\mathrm{AGE}(\theta,t)$, which expresses masses of crustal domains formed at age θ ago and preserved till age t. The flux of liquid silicate from sf into the crust is determined by $\mathrm{AGE}(\theta,t)$ for $t=\theta$. This flux and the fraction of liquid silicates in sf (see Section 7.3) determine the total influx, which is equal to the sum of two fluxes: from the mantle wedge and from the oceanic crust, and we used here the same flux ratio as was inferred from Th–U–Pb modeling (see (12) in Kramers and Tolstikhin, 1997). The difference between the total influx and the flux of liquid silicates into the crust gives the flux of solid silicate from sf into the mantle.

The crustal growth curve, $\mathrm{d}M_{\mathrm{CC}}/\mathrm{d}t$, is a free parameter, which should be constrained by modeling (see Section 7.3). Then the flux of eroded material is the difference $\mathrm{AGE}(t=\theta,T)-\mathrm{d}M_{\mathrm{CC}}/\mathrm{d}t$ (see Eqs. (17), (18) and Fig. 6 in Kramers and Tolstikhin, 1997). In our simple model with just one crustal reservoir, the composition of the eroded material is the same as the bulk crustal composition at a given time (Section 6.2). The degassing flux from the crust into the atmosphere is described by the product of the degassing coefficient $L_{\mathrm{COC,ATM}}$ [Gyr^{-1}] and the total amount of volatile species ${}^{i}\mathrm{N}_{\mathrm{COC}}$ [at] in the crust, $\mathrm{L}_{\mathrm{COC,ATM}}\times{}^{i}\mathrm{N}_{\mathrm{COC}}$, and the recycling flux of atmospheric rare gases into the mantle is described in a similar way.

5. Accreting materials: "terrestrial chondrite"

Even though prototerrestrial material (or "terrestrial chondrite", a term proposed by M. Drake) cannot be wholly identified with any known type of chondritic meteorites, we use in this study chondrite-like initial elemental and isotopic abundances of the involatile elements Sm, Nd, Lu, Hf, W, U, Th, Sr as well as involatile siderophile elements (Table 1). Rb–Sr and K–Ar systematics are also included: even though Rb and K are moderately volatile elements, their terrestrial initial abundances are reconstructed via K/U and Rb/U ratios, which are well constrained in the Earth, and absolute initial concentration of involatile uranium. Assuming such a starting material allows to evaluate, in spite of uncertainties, whether both present-day in-

ventories and evolution trends can be satisfied for an Earth model with whole mantle convection.

For the absolute initial concentrations of the highly volatile rare gases in the "terrestrial regolith" that partially formed D″, only upper limits can be given: they should not be higher than those observed in solar-noble-gas-rich meteorites and the lunar regolith: $^{3}He_{SIN} < 1 \times 10^{-5}$ cc STP g^{-1} (Benkert et al., 1993; Pedroni and Begemann, 1994; Busemann et al., 2000). The relative initial abundances of light rare gas isotopes (He, Ne and Ar) are considered as solar, by analogy with solar implanted gases and taking into account the

Table 2
Calculated abundances of noble gas species and parent elements in principal terrestrial reservoirs

N	Parameter	Dimensions	D″	Mantle	Cont. crust
			a	b	c
1	Mass	g	2.31×10^{26}	3.74×10^{27}	2.26×10^{25}
2	U	ppb	71.5	7.7	1300
3	^{3}He	cc STP/g	2.5×10^{-7}	6.7×10^{-11}	5×10^{-12}
4	$^{4}He/^{3}He$	Ratio	2.8×10^{3}	8.5×10^{4}	1×10^{8}
5	^{40}Ar	cc STP/g	6.7×10^{-5}	2.3×10^{-6}	1.7×10^{-4}
6	$^{40}Ar/^{36}Ar$	Ratio	2.9×10^{3}	4.8×10^{4}	
7	^{130}Xe	cc STP/g	1.4×10^{-11}	3.5×10^{-14}	
8	$^{129}Xe/^{130}Xe$	Ratio	17.5	7.6	
9	$^{136}Xe/^{130}Xe$	Ratio	2.47	2.54	
10	$^{136}Xe(U)$	cc STP/g	2.3×10^{-13}	1.2×10^{-14}	1.1×10^{-12}
11	$^{129}Xe(I)/^{136}Xe(U)$	Ratio	664	4.5	
12	$^{136}Xe(Pu)/(^{136}Xe(U)+^{136}Xe(Pu))$	Ratio	0.97	0.28	0.02

Because of severe mantle degassing (Section 7.2) rare gases are treated as highly incompatible elements with solid/melt bulk partition coefficient=0.001 for all rare gas species. In the course of formation of the oceanic crust all rare gases are transferred from the respective melt flux into the atmosphere.

The melt fraction in the mantle fractionation zone is a linearly decreasing function of time from 0.3 at $t=0$ (start of accretion) till 0.1 (at present); it is constant in the subduction fractionation zone varying from 0.01 to 0.008 in different versions of the model. Numbers refer to row "*N*":

(1a) The initial model D″ mass is 2.46×10^{26} g, so only 6% of the D″ mass has been entrained by mantle convective flow in the course of Earth history. Taking into account the model pm/D″ mass ratio, 0.2, then the inferred amount of prototerrestrial materials used to maintain rare gas flux through the mantle (since 4.5 Gyr ago) is $\leq 0.05\% \times M_{EARTH}$. This value is valid for rare gas systematics and it is slightly below the respective estimate for the noble metals, $\leq 0.1\% \times M_{EARTH}$. Noble metals, however, can be reconciled without a flux from D″ (Section 7.1).

(2abc) The crustal concentration of U is equal to that suggested by (Weaver and Tarney, 1984) and is ~10% below the estimate of Rudnick and Fountain (1995). The mantle U concentration is the same as that derived from U–Th–Pb modeling by Kramers and Tolstikhin (1997) for the depleted upper mantle. The K/U mass ratio in all reservoirs is 12,000 (adjusted to reconcile the amount of atmospheric ^{40}Ar); the ratio is similar to that proposed by (Jochum et al., 1983); $^{232}Th/^{238}U=3.9$ in all reservoirs, the second lead paradox is not addressed in this contribution (Kramers and Tolstikhin, 1997).

(3a) This concentration of $^{3}He_{DDP}$ corresponds to $^{3}He_{SIN}=1.25 \times 10^{-6}$ cc STP g^{-1} implanted in the "terrestrial regolith".

(4a) All ratios of $^{4}He/^{3}He$ and $^{21}Ne/^{22}Ne$ observed in plume-derived rocks (minerals) and fluids (including the very low ones, Section 6.3.1) can be explained by mixing of D″, plume-source, and mantle rare gases.

(4b) Slightly above $^{3}He_{BLM} \approx 3 \times 10^{-11}$ as inferred for the MORB-source mantle from the ^{3}He inventory in the oceans (Marty and Tolstikhin, 1998).

(5a) Portion of terrestrial ^{40}Ar generated and preserved in D″ approaches 24% of the terrestrial inventory and 55% of its inventory in the silicate earth.

(5b and 6b) This concentration results mainly from $^{36}Ar_{ATM}$ recycling. Without recycling the model ^{36}Ar concentration in the mantle is much lower, $^{36}Ar_{BML}=6.2 \times 10^{-12}$, and model the mantle $^{40}Ar/^{36}Ar$ approaches 370,000. Air recycling has little effect on the ^{40}Ar concentration of the mantle.

(5c) The crustal degassing constant applied is $L_{COC,ATM}=0.5\ Gyr^{-1}$. $^{40}Ar^{*}$ that survived in this degassing (weathering, metamorphism, etc.) in the continental crust corresponds to 6% of the total terrestrial $^{40}Ar^{*}$. The mean K–Ar age of the crust is 1.7 Gyr, slightly less than Sm/Nd age of 2.2 Gyr.

(5abc) Along with the atmospheric $^{40}Ar=3.69 \times 10^{22}$ cc STP these values give 6.55×10^{22} cc STP, which is 88% of the total ^{40}Ar generated by terrestrial potassium; 12% of terrestrial ^{40}Ar had been lost along with $^{129}Xe(I)$ and $^{136}Xe(Pu)$.

(7a) $^{130}Xe_{DDP}$ is determined by the model-derived concentration of $^{129}Xe(I)_{DDP}$ and the $^{129}Xe/^{130}Xe$ ratio observed in CO_2 gas xenon (see 8a). In turn, $^{130}Xe_{DDP}$ determines the mixing proportion of Q (Busemann et al., 2000) and solar (Anders and Grevesse, 1989) initial rare gas components. The model-derived ratio of $^{130}Xe_{Q}/^{130}Xe_{SIP}=340$, and the ratio of $^{36}Ar_{Q}/^{36}Ar_{SIP}=0.39$.

(8a) Similar to the ratio of ^{129}Xe over the light-isotope-enriched fraction of ^{130}Xe observed in CO_2 gas xenon (Tolstikhin and O'Nions, 1996).

(8b and 9b) These ratios fit the observed $^{129}Xe/^{130}Xe$ versus $^{136}Xe/^{130}Xe$ mantle correlation (Tolstikhin and O'Nions, 1996).

(12a) Xe(Pu) is the principal fission Xe component in D″.

(12b) Contribution of Xe(Pu) as proposed by Kunz et al. (1998).

solar-like light-noble-gas signatures in the mantle. Chondrite-like material, the principal constituent of D″, could preserve Q-type noble gases with enhanced abundances of heavy species. Non-solar noble gas abundance patterns in the Earth's mantle (with high Xe/Ar) have been discussed by Harper and Jacobsen (1996) (who argued for Q gases in the mantle), and Porcelli and Wasserburg (1995). Mixtures of solar-like and Q components are a general feature of chondritic meteorites, in particular enstatite chondrites (Busemann et al., 2003). These have the same O-isotope abundances as terrestrial materials (Clayton, 2003) and formed near the Earth's feeding zone, as follows from their Mn–Cr isotope systematics (Shukolyukov and Lugmair, 2004). Ratios of Q gases to solar implanted nuclides (SIN) in meteorites vary from an almost pure Q-component in carbonaceous chondrites (e.g., Allende CM2, Busemann et al., 2000), to pure SIN (e.g., Acfer H3-6, Pedroni and Begemann, 1994). A mixture between Q- and solar-implanted gases is a suitable starting composition as discussed by Kramers (2003). The proportion of mixing is an unknown parameter constrained by modeling (Section 7.3.1 and Table 2 below present the calculated noble gas abundances, which yield the solution of the model).

Ne isotope systematics are not included because, as Honda et al. (1993) have shown, they generally corroborate helium isotope data. Nevertheless we discuss below some important observations on very primitive neon isotope composition in Iceland basalts (Section 6.3.1).

6. Principal terrestrial reservoirs, present-day characteristics and evolutionary trends

The accessible portion of the Earth (i.e. excluding D″ and core) in our model consists of three major long-lived complementary reservoirs: (i) a large incompatible-element-depleted degassed mantle, treated here as one convecting and relatively homogeneous reservoir, (ii) a small enriched heterogeneous continental crust (also treated as a single reservoir), and (iii) a volatile-bearing atmo-hydrosphere. In the following Sections (6.1–6.3) we discuss parameters of these reservoirs that are used as target values in modeling.

6.1. The siderophile element abundance pattern in the mantle

The mantle abundances of siderophile elements display a specific pattern. The groups of moderately and highly siderophile elements show, within themselves, chondritic relative abundances, but with different depletion factors, $\sim 8 \times 10^{-2}$ for moderately and $\sim 3 \times 10^{-3}$ for highly siderophile metals. It is important that this grouping is in apparent accord with the degree of siderophile behaviour of the elements: moderately and highly siderophile elements constituting the groups are progressively more depleted, and this would be consistent with equilibrium metal–silicate fractionation during the core formation process. However, within each group the observed chondrite-normalised abundance pattern is flat, thus portraying element ratios consistent with accreting not-yet-fractionated materials. Also the observed abundances exceed those predicted from single-stage equilibrium fractionation for most of these elements, especially so for noble metals.

The depletion factors yield important clues about the segregation process. These factors are different from the predicted outcome of a single-stage metal/silicate equilibrium process, but they are in accord with models that combine equilibrium partitioning between metal and silicate fractions in continuous core segregation (contemporaneous with accretion) with substantial mixing of chondrite-like accreting and already metal-free silicate material. Moreover, a continuous multi-stage core segregation mechanism directly follows from the standard Earth accretion model: generally planetary embryos were already differentiated before they impacted the growing Earth. After each collision the metal cores of the impactor and target could partly react again with the silicate mantle, and partly combine without re-equilibration, as pointed out by Karato and Murthy (1997). Therefore in this contribution we use a model that envisages continuous core segregation during accretion (Stevenson, 1990), post-impact mixing of fractionated and unfractionated materials followed by equilibrium metal–silicate partitioning (Azbel et al., 1993).

6.2. Sm–Nd, Lu–Hf and Rb–Sr isotopic systematics

MORB magmatism, generating $\sim 6 \times 10^{16}$ g of basaltic melt per year (Crisp, 1984), causes major mantle fractionation and degassing. Mantle fractionation through time is recorded by several isotope systematics and we use Sm–Nd and Lu–Hf to model this record. Even though a large amount of accurate measurements of Sm/Nd ratio and Nd isotopic compositions in MORB samples is available, the problem of how representative they are is still open. Attempting to resolve this problem, Su (2002) compiled average trace element and isotope abundances for ridge segments of a given length. The respective total-net average (for ~300 ridge segments, ~1300 measurements) derived from his com-

pilation is ε(Nd) = 8.9 ± 1.6. Intersect of this ε(Nd) and regression of the terrestrial array shown in Fig. 1 gives the present-day mantle ε(Hf) = 17.

In contrast to the well-defined Nd and Hf isotope compositions, the observed MORB concentrations of Sm, Nd, Lu and Hf as well as Sm/Nd and Lu/Hf ratios vary because the REE fractionate during MORB extraction. Therefore only estimates derived from melting models are available for the MORB-source mantle: Nd~0.8 ppm, Sm/Nd ≈ 0.37, Nd/Hf ≈ 4 and Lu/Hf ≈ 0.27 (e.g., McKenzie and O'Nions, 1991; Chauvel and Blichert-Toft, 2001; see Table 3).

The plot of initial $^{143}Nd/^{144}Nd$ ratios in mantle rocks versus age (Nägler and Kramers, 1998, see data sources in their paper) shows the mantle Nd isotope evolution, which also constrains the model solution (Fig. 3). The initial Nd isotope composition of the solar system is not known very precisely and there is some discussion whether it conforms to the CHUR model or is slightly, e.g. by +1 ε(Nd) higher. If a CHUR initial ε(Nd) is chosen, the most ancient rocks indicate a depletion of their source, which would imply early mantle fractionation.

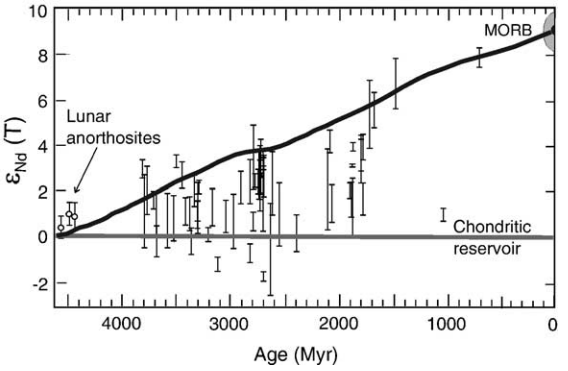

Fig. 3. Initial Nd isotope compositions in mantle-derived rocks (after Nägler and Kramers, 1998, see sources of data in their contribution) and the whole-mantle ε_{Nd} evolution curve of our reference solution. Of the total ε_{Nd} value of +9 of the present mantle, +5 is due to D″ and +4 to the continental crust (see text).

Regarding Rb–Sr isotope systematics, the compilation by Su (2002) gives a reliable $^{87}Sr/^{86}Sr$ = 0.7028 ± 0.0004 for the present-day MORB source, which is indistinguishable from an earlier estimate by Ito et al. (1987). No such agreement exists for the proposed concentrations of the parent and daughter

Table 3
Output parameters for Sm–+Nd, Lu–Hf and Rb–Sr isotope systematics

N	Parameter	Dimension	D″	Mantle	Cont. crust
			a	b	c
1	Mass	g	24.47	372.86	2.26
2	Nd	ppm	5.4	0.86	22.6
3	$^{147}Sm/^{144}Nd$ (Sm/Nd)	Ratio	0.17 (0.28)	0.22 (0.37)	0.115 (0.19)
4	ε(Nd)	Ratio	−15	9	−17
5	Hf	ppm	1.150	0.203	4.370
6	$^{176}Lu/^{177}Hf$ (Lu/Hf)	Ratio	0.021 (0.15)	0.040 (0.29)	0.012 (0.087)
7	ε(Hf)	Ratio	−35	16.4	−20
8	Sr	ppm	83	14	360
9	$^{87}Rb/^{86}Sr$ (Rb/Sr)	Ratio	0.092 (0.03)	0.045 (0.015)	0.28 (0.1)
10	$^{87}Sr/^{86}Sr$	Ratio	0.7048	0.7029	0.7102

Solid/melt bulk partition coefficients:
In the mantle fractionation zone (mf, Fig. 2B) Nd—0.025, Sm—0.065, Hf—0.0385, Lu—0.19, Sr—0.033, Rb—0.001.
In subduction-related fractionation (sf, Fig. 2B) Nd—0.03, Sm—0.065, Hf—0.0385, Lu—0.145, Sr—0.033, Rb—0.0002 (see text for discussion). (3abc and 6abc and 9abc) Mass ratios are shown in brackets.
(2c and 3c) Calculated crustal Nd concentrations and Sm/Nd, Hf/Nd ratios are within the range of estimates suggested by different authors (see Table 11 in Rudnick and Fountain, 1995). Exactly the same crustal Sm/Nd ratio was inferred by Nägler and Kramers (1998) for the layered mantle model; their model upper mantle (i.e., reservoir complementary to the continental crust) was 1×10^{27} g, by a factor of 4 larger than D″.
(3b) Indistinguishable from the ratio derived by Chauvel and Blichert-Toft (2001) from MORB source mantle melting models.
(4bc and 7bc) The ε-coordinates of mantle and crustal endmembers lie on the Hf–Nd isotope terrestrial array regression line (Fig. 1).
(6b) Same as inferred by Blichert-Toft and Arndt (1999) for the source of ancient komatiites. Chauvel and Blichert-Toft (2001) inferred Lu/Hf = 0.28 from MORB source mantle melting models.
(6c) The model derived $^{176}Lu/^{177}Hf$ is indistinguishable from the average ratio in sedimentary rocks, 0.0117, which could be a proxy for the continental crust (see Table 2 in Vervoort et al., 1999).
(8c) As recommended by Rudnick and Fountain (1995).
(9bc) Corresponds to Rb/Sr ratios 0.015 and 0.1 for the mantle and continental crust, respectively. The latter value is between those suggested by Jacobsen and Wasserburg (1979) and Taylor and McLennan (1985).
(10b) Corresponds to the MOR-segment-arranged data-base (307 MOR segments, totally 1300 ratios) of Su (2002), 0.70285 ± 0.00039 (± 1σ).
(10c) Within the limits suggested for the total continental crust by Jacobsen and Wasserburg, 1979).

elements: White and Schilling (1978) suggested Rb=0.15 ppm and Sr=25 ppm, whereas Workman and Hart (2005) derived much lower values of 0.05 and 7.7 ppm, respectively, from their modeling (see discussion in Section 7.3.2).

The continental crust is treated as a single reservoir in this study. This choice appears to be reasonable for Lu–Hf and Sm–Nd systematics, because the Nd and Hf isotope compositions in magmatic, metamorphic and sedimentary rock-types form a coherent terrestrial array indicating the two principal end-members involved: the continental crust and the depleted MORB-source mantle (see Fig. 1). According to Vervoort et al. (2000) "the lower crust appears to be broadly similar to upper crustal samples" and we used respective estimates by Goldstein and Jacobsen (1988) as the mean target crustal values: $Nd_{CC}=22\pm5$ ppm, $Sm/Nd_{CC}=0.21\pm0.02$ and $\varepsilon(Nd)_{CC}=-17\pm5$. These values are in overall agreement with the sedimentary rock data presented by Vervoort et al. (1999). The Hf–Nd terrestrial array relates isotopic Hf and Nd characteristics of the two reservoirs and we infer the target Hf compositions of mantle and crust using those for Nd (above) and the array regression (Vervoort et al., 1999, 2000).

Note that the above crustal concentration of Nd gives a total $Nd_{CC}=\sim5\times10^{20}$ g, which is about 1/6 of the total amount in the (depleted) mantle. The mantle appears to be the major REE bearing terrestrial reservoir, and therefore its Sm–Nd systematics are not very sensitive to the crust–mantle erosion-recycling flux. As a result the difference between $\varepsilon(Nd)=-17\pm5$ (mean for the upper crust) and -11 ± 4 (sediments) reflecting preferential erosion of relatively young rocks (Goldstein et al., 1984) is not very important for this work and we assume the Nd of the crustal erosion flux to have the bulk crust isotope composition.

For the sake of simplicity one crustal reservoir is also used for modeling Rb–Sr systematics even though Rb/Sr ratios of the lower and upper crustal reservoirs are quite different, ~0.03 and ~0.3, respectively (Rudnick and Fountain, 1995), generating corresponding differences in $^{87}Sr/^{86}Sr$ ratios in these sub-reservoirs, ~0.705 and ~0.720, respectively (Goldstein and Jacobsen, 1988; Allegre et al., 1996; Downes et al., 1997). Taking into account that strontium concentrations in the lower and upper crust are similar, then the mass balance gives the target whole-crust value ~0.710.

As Sm–Nd and Lu–Hf systematics concern lithophile refractory elements, mass balance considerations such as that of Section 2.2., with D″ added, can be applied to them to assess directly whether the layered mantle paradox could be solved by a D″ reservoir as sketched in Section 3. This is illustrated for the case of Sm–Nd:

$$M_{CC}Nd_{CC}\varepsilon(Nd)_{CC}+M_{DM}Nd_{DM}\varepsilon(Nd)_{DM}+M_{DDP}Nd_{DDP}\varepsilon(Nd)_{DDP}=(M_{CC}+M_{DM}+M_{DDP})\varepsilon(Nd)_{BSE} \quad (3)$$

If $M_{CC}+M_{DM}+M_{DDP}=M_{\text{silicate Earth}}$, the masses of the reservoirs are taken from Table 2 and a typical value for komatiites (5 ppm) is used for the Nd concentration of D″, the resulting value for $\varepsilon(Nd)_{DDP}=-15.8$. This is almost as low as the value for the continental crust (−17). But if the D″ reservoir was isolated in earliest Earth history, it corresponds to a $^{147}Sm/^{144}Nd$ ratio of 0.165. This ratio is only16% enriched relative to chondrites, or primitive mantle, which is reasonable for mafic volcanics. Thus the D″ hypothesis appears reasonable from Sm–Nd systematics. In the forward modeling below, Nd and Sm concentrations in D″ follow from known values of partition coefficients, and it yields results quite similar to this simple mass balance.

6.3. Terrestrial rare gas isotopic systematics

The mantle rare gas systematics have already been discussed in Sections 2.1 and 2.2; some comments are also given as notes to Table 2. Here we highlight two issues only.

6.3.1. Almost-solar neon in a solar-rare-gas source

Dixon et al. (2000) discovered low $^{21}Ne/^{22}Ne$ ratios, almost indistinguishable from the solar value, in Iceland basalts. These low $^{21}Ne/^{22}Ne$ ratios can be translated into a $^{4}He/^{3}He$ ratio in the source, if the initial abundances were solar ($^{21}Ne/^{22}Ne_{SOS}=0.033$ and the ratios as in Table 1) and the maximum contribution of nucleogenic $^{21}Ne^{*}$ in the source is given by $^{21}Ne/^{22}Ne_{DDP}=0.0375$ (p. 318 in Dixon et al., 2000):

$$^{4}He/^{3}He_{DDP}=\left(^{4}He/^{3}He_{SOS}+\left(^{21}Ne/^{22}Ne_{DDP}-Ne^{21}/^{22}Ne_{SOS}\right)\times\left(^{4}He/^{21}Ne\right)^{*}\times\left(^{22}Ne/^{3}He\right)_{SOS}<15,000 \quad (4)$$

where the $(^{4}He/^{21}Ne)^{*}$ ratio is 1.5×10^{7} (Leya and Wieler, 1999). Even though the Th–U–Ne trio is not included in the present modeling, this important fingerprint of very primitive Ne in the Earth now constrains Th–U–He systematics: the model-derived present-day $^{4}He/^{3}He$ ratio in the source of this solar-like noble gas

should not exceed the above value. Also, Matsumoto et al. (2002) observed a low $^{4}He/^{3}He$ ~10,000 in ancient komatiite. This is lower than the MORB value ($^{4}He/^{3}He = 86{,}000$) by almost an order of magnitude.

These observations present convincing evidence for low time-integrated (U and Th)/^{22}Ne and (U and Th)/^{3}He ratios, at least a factor of ~100 lower than MORB, in the source reservoir of mantle rare gases (if this reservoir was formed early in Earth history). Such very low ratios could hardly have resulted from U and Th depletion, because rocks with U < 1 ppb have almost never been observed. Also other isotopic systematics do not point to the existence of a reservoir that is more depleted in incompatible elements than the MORB-source mantle. Such a reservoir would also have other specific fingerprints, e.g., very low Rb/Sr and therefore low $^{87}Sr/^{86}Sr$ ratios. This is contrary to observations: ^{3}He-rich plume-related rocks generally show a more radiogenic Sr than normal MOR basalts. Therefore a reservoir enriched in solar rare gases remains as a plausible explanation. This has previously been concluded, e.g. by O'Nions and Oxburgh (1983), Kellogg and Wasserburg (1990), Porcelli and Wasserburg (1995), Tolstikhin and Marty (1998), and Moreira et al. (2001) (see Section 2.2); our conclusion differs from previous ones in that we regard only D″, and not the whole lower mantle, as such a reservoir.

The observed spectrum of rare gas isotope compositions in mantle rocks of various ages could result from mixing of the almost-solar rare gases that migrated from their host reservoir into the MORB-source mantle with its radiogenic component. In the course of such mixing, apparent "decoupling" of He and Ne isotope systematics could occur (e.g., Dixon et al., 2000; Dixon, 2003), probably because of different $^{3}He/^{22}Ne$ ratios in the solar-noble-gas source (~2) and in the mantle (~10). This difference could result from the slightly better retention of helium, which is more soluble in melts than neon, in the course of continuous mantle degassing (see Azbel and Tolstikhin, 1990, for discussion and modeling of possible mechanism of increasing of He/Ne in the mantle through time). It is also possible that the better helium diffusivity (compared with other rare gases) plays a role.

Irrespective of these details, the fundamental features that must be reproduced by any adequate model of light-rare-gas mantle systematics are almost solar He and Ne isotope compositions in a source that has extremely low (U and Th) over ^{22}Ne (or ^{3}He) ratios. This implies relatively high ^{3}He and ^{22}Ne concentrations. Table 2 shows how the values are produced by the reference solution of our model.

6.3.2. The role of the continental crust in the terrestrial rare gas inventory

In the continental crust, rare gas signatures of mantle provenance are overshadowed by the production of radiogenic (nucleogenic) species and further affected by noble gas loss from crustal rocks. As a given crustal domain becomes more and more mature, generally within ~0.5 Gyr after magmatism has ceased, the contribution of mantle rare gases becomes almost invisible (Polyak and Tolstikhin, 1985). Therefore the crust as a whole is considered as a source of radiogenic gases only. In this respect there is no principal difference between lower and upper crustal reservoirs and within the frame of the rare gas model one crustal reservoir, the whole crust, is appropriate for modeling. Moreover, because of the relatively young mean age of the crust and because it lost part of its radiogenic rare gases (via metamorphism, weathering, diagenetic processes, etc.) the continental crust is also unimportant as a reservoir of radiogenic rare gas nuclides. However, it is the principal store of the parent elements Th, U, I, and K, which are all strongly incompatible. Their transfer from the mantle and resulting mantle depletion reduces the production of radiogenic nuclides in the mantle and thus affects the mantle noble gas signature; this transport, generation and degassing of radiogenic rare gases are therefore included in the model.

7. Results of modeling and discussion

7.1. Accretion and core segregation (4.568–4.4 Ga ago)

Accretion was by far the most intense period in earth history, which is reflected by the large fluxes seen in Fig. 4. The accretion mass flux is constrained by the mass of the Earth and the accretion time scale, i.e., the time interval between the formation of the solar system (assigned as $t \equiv 0$) and the Giant Impact envisaged in the model from a priori data. The impact is seen in Fig. 4 as a step in the accretion curve and a spike in the mantle fractionation rate. Hf–W systematics constrain the timing of this event at 30–35 Myr after solar system formation (Kleine et al., 2002; Schoenberg et al., 2002; Yin et al., 2002).

After the Giant Impact, accretion slows down. In the model its tailing-off is constrained by the mass of chondritic material in the D″ reservoir and the time interval of D″ formation. The duration of this interval (Fig. 4) is dictated by mantle xenology, namely, by the upper limit of $^{129}Xe(I)/^{136}Xe(Pu)$ ratio in mantle xenon, (e.g., Kunz et al., 1998; Caffee et al., 1999).

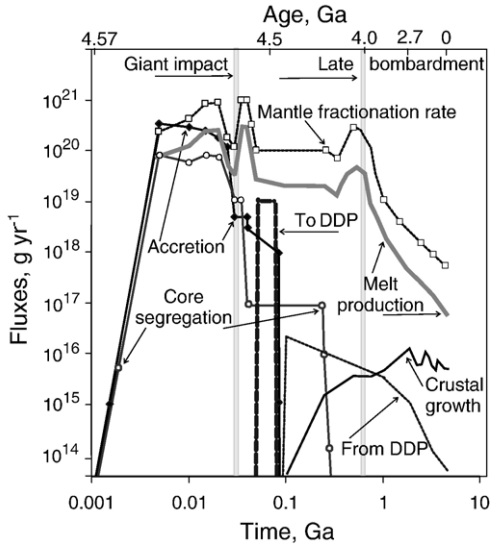

Fig. 4. Mass fluxes inferred from the reference model solution. The accretion mass flux is constrained by the earth mass and earth accretion time scale (30 Myr, from Hf–W systematics, e.g., Kleine et al., 2002), and by the mass of D″ (similar to the present-day value, Table 2), its formation time scale (70 Myr, from mantle xenology, e.g., Kunz et al., 1998) and the fraction of chondritic material in D″ (0.2, Table 1); correspondingly, the flux of prototerrestrial material constitutes 1/5 of the total flux into D″. The core segregation mass flux is constrained by core mass and accretion time scale, with a tailing off constrained by noble metal abundances in the mantle (Section 6.1). The melt production in the mantle is constrained by the core segregation rate during the first ~200 Myr and by mantle xenology afterwards (Sections 6.1 6.2 and 6.3.1); this flux in turn constrains the mantle fractionation rate via the melt fraction coefficient (Table 2). The mass flux from D″ is constrained by mantle rare gas systematics (Section 6.3.1). Crustal growth (right bottom corner of the Figure) and erosion (not shown) fluxes are adopted from the Th–U–Pb model (Kramers and Tolstikhin, 1997).

The total flux of the basaltic crust along with the terrestrial regolith is then constrained by the mass of D″ (Fig. 4). The abundances of the trace elements of interest in the 80% oceanic crust component of D″ are determined by their abundances in prototerrestrial material (Table 1), by the melt fraction in the mantle fractionation zone (see notes to Table 2), and by the respective partition coefficients (see notes to Tables 2 and 3). The 20% component of non-fractionated chondrite-like material in D″ contains siderophile elements in chondritic relative proportions as well as Q and solar implanted rare gases as shown in Tables 1 and 2 and discussed in the respective notes.

Because large differentiated planetesimals (or embryos) were formed within a short time interval, e.g., ~5 Myr after solar system formation (Carlson and Lugmair, 2000), the mass flux of metal into the core starts simultaneously with accretion in this model, which here describes a collective process in many planetesimals. The abundances of siderophile elements in the collective mantle determine the interrelationships between mantle fractionation and core segregation fluxes (Fig. 4) and the fraction of metal in the mantle fractionation zone (mf). The fraction of silicate melt in this zone decreases through geological time, from 0.3 during the late stage of accretion (4.5 Ga ago) to 0.1 at present (Section 7.3).

The reference model solution reveals depletion of mantle siderophile elements in three distinct stages (Fig. 5). During the first major stage of accretion (0 to 30 Myr) two contemporaneous processes govern the depletion: accretion of chondritic material, which adds the elements to the earth's mantle, and partitioning of the elements into a metal phase, the flux of which into the core removes the elements from this reservoir. Because a relatively large fraction of metal is still available at that time, all siderophile elements are (almost) quantitatively partitioned into the metal in mf, and the similarity of the abundances for highly and moderately siderophiles, ~0.2 (Fig. 5), simply reflects mixing of processed metal-free mantle material with newly arrived metal-bearing bodies.

The Giant Impact and its effects constitute the second stage: the most intense fractionation rate, a large metal fraction, and a low accretion flux afterwards all ensure efficient depletion of all siderophile elements immediately after the impact (Fig. 5).

During the third stage the mass flux into the core still continues (i.e., a flat tail of the core segregation mass flux is seen in Fig. 4), but accretion is slow and then ceases. Therefore the metal fraction in the mantle fractionation zone decreases and moderately siderophile

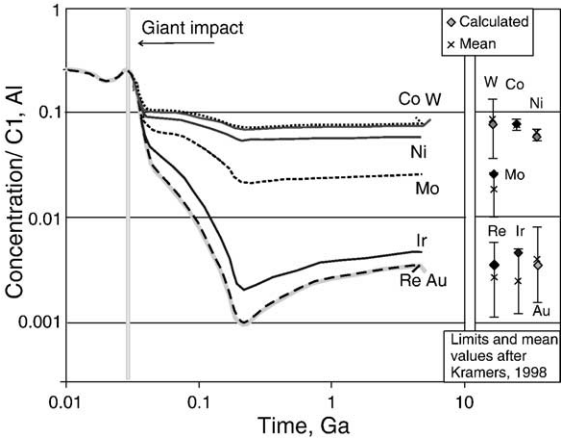

Fig. 5. Evolution of abundances of involatile siderophile elements in the mantle. See text for discussion.

elements are partitioned into the metal and removed from the mantle (into the core) less efficiently than highly siderophile elements. During this stage the moderately siderophile elements are fixed in the mantle, and highly siderophile elements are further depleted.

In the course of geological time, the noble metal abundances in the mantle gradually increase by entrainment of D″ material with enhanced abundances of all siderophile elements, ~0.2 (Table 1). This process is not an intrinsic feature of the continuous core segregation model: A solution for the siderophile elements can be obtained without a D″ reservoir (Kramers, 1998). However, the late influx of material with a chondritic siderophile element pattern and transfer of this material from the Earth surface into the mantle are indeed unavoidable. In other words, the model solution for siderophile elements does not necessarily require the existence of a D″ reservoir, but it illustrates how and from which material this reservoir could be formed.

7.2. The Hadean era (4.4 to 4 Ga ago)

In the reference solution, the rate of mantle fractionation and the attendant flux of silicate melt (enabling degassing) during the Hadean era are up to 3 orders of magnitude greater than the present-day value. Extremely efficient mantle degassing is a very robust result, constrained by the low ^{136}Xe(Pu)/^{136}Xe(U) ratio in mantle xenon. This may be illustrated by comparison of the observed and closed system ratios as discussed in Section 2.1. Because "complete" early degassing (as well as "complete" subsequent retention, Section 2.1) are obviously unrealistic, our model envisages a finite degassing flux (defined as the rate of mantle melt production). We consider that this flux was intense in early Earth history and removed most xenon from the mantle. We assume that this flux decreased first rapidly and then gradually through time, along with the melt production rate. Taking into account that, at least after the late bombardment event at ~4 Ga ago, no significant energy input from external sources (impacts) into the earth is expected, that radioactive isotopes are decaying and that the earth is gradually releasing energy acquired during the accretion and core segregation, this assumption appears to be reasonable. We varied the rate of mantle melt production and degassing through time until the calculated mantle ^{136}Xe(Pu)/^{136}Xe(U) ratio approached the observed value (Table 2; see Section 2.1.). The effective mantle retention coefficient (the abundance of a stable rare gas isotope in the present-day mantle divided by its initial abundance 4.57 Gyr ago) is of the order of 10^{-10}, indicating extreme mantle degassing. A similar value was derived by Tolstikhin and Marty (1998, see Fig. 6 in their contribution).

The discovery of Xe(Pu) in ancient terrestrial zircons and the confirmation of the initial chondrite-like Pu/U ratio (Turner et al., 2004) strengthens the reliability of the conclusion on extreme mantle degassing during early Earth history. As Xe(Pu) is almost invisible in the present day mantle, it must have been degassed.

Because mantle convection governs post-accretion melt generation and degassing, the high rate of degassing during the first almost 1 Gyr of Earth history (Fig. 4) indicates vigorous convection within this reservoir. Energy released in the course of accretion and core formation and still available in the Earth was probably the major moving force of this early intense convection and degassing. However the degassing rate could also be enhanced by late impacts occurring between 4.5 and 3.9 Gyr ago, that disrupted the crust leading to uplift of hot mantle material, melting and degassing. Such effects could be considerable even if the total flux of impactors was small (e.g., p. 189 in Pritchard and Stevenson, 2000). Correspondingly, in this model we consider that the late bombardment caused intense melt production and degassing, but had little effect on terrestrial mass balance.

As mentioned in the Introduction, the sources of atmospheric rare gases and the processes responsible for their elemental and isotopic fractionation are beyond the frame of this contribution. The only result we wish to highlight here is that the reference solution predicts late loss of Xe(Pu) from the atmosphere, at ~ 0.25 Gyr after solar system formation. This time was obtained via adjustment of the duration and intensity of the dissipation flux (Fig. 2) to reconcile calculated and observed abundances of radiogenic Xe isotopes in the atmosphere. A similar time scale follows from a simple two-stage model. The amount of live ^{244}Pu still present in mantle+crustal reservoirs at a time t after solar system formation would afterwards produce

$$^{136}\mathrm{Xe}\,(\mathrm{Pu}) = 0.8 \times B_{244} \times Y_{244} \times {}^{244}\mathrm{Pu}_{\mathrm{INI}} \times \exp(-\lambda_{244} t) \quad (5)$$

where all parameters are from Table 1. B_{244} and Y_{244} are the fission branching ratio and the ^{136}Xe yield (Note 20 of Table 1). The coefficient 0.8 takes into account that an early-separated D″ had incorporated and stored ~20% of all incompatible elements (including Pu) in earliest Earth history. For t=0.22 Gyr, the calculated value is equal to the amount of ^{136}Xe(Pu) presently in the Earth's atmosphere (~1.27×10^{15} cc STP), assuming primitive "U–Xe" as the progenitor of air Xe (see

Azbel and Tolstikhin, 1993). Because both crustal and mantle reservoirs contain at present negligible amount of ^{136}Xe(Pu) compared with the atmosphere, the above time corresponds to the end of Xe loss from the Earth—atmosphere system.

The difference between the two estimates (resulting mainly from different degassing rates in the two models) is very small compared to the real uncertainties: the initial abundance of ^{244}Pu could vary within a factor of ~2 and the atmospheric amount of ^{136}Xe(Pu) is highly dependent on the poorly known progenitor of atmospheric xenon. With the present state of the art, the time scale for the end of atmospheric Xe loss could vary from ~100 Myr until as late as ~ 500 Myr after solar system formation, i.e., until the late bombardment.

Within the frame of the reference solution, a small part of radiogenic ^{40}Ar* (~12% of its total production) must have been lost along with Xe.

7.3. Geological evolution (4 Gyr ago until present)

The rate of mantle melt production and degassing decreases smoothly through time to its known present-day value. This rate and the mass flux from the D″ reservoir are constrained by mantle rare gas isotope signatures. The rate of crustal growth, the crustal age distribution function and mass fluxes into and from the crust are taken from the reference solution of the Th–U–Pb model, which carries the most severe constraints on crustal growth and recycling (see Fig. 7 and 10 in Kramers and Tolstikhin, 1997).

7.3.1. Model-derived rare gas and parent element abundances in D″, the MORB-source mantle, and the crust

As already highlighted by Tolstikhin and Hofmann (2005), the D″ layer could be an important reservoir of radioactive heat-generating elements, U, Th, and K: the model-derived abundances of these elements in D″ are ~20% of the BSE amounts. The high abundance of K means that the amount of ^{40}Ar* hidden in D″ allows a terrestrial inventory of ^{40}K–^{40}Ar* systematics with K/U_{BSE}=12,000 (Table 2). The abundances of light solar rare gases are so high that even with enhanced concentrations of U and Th, D″ is characterised by a low (U and Th)/^{3}He ratio and an almost-solar isotope composition of He (Table 2). The ^{3}He concentration in the model "terrestrial regolith" is about 100× lower than those observed in lunar ilmenites (Benkert et al., 1993) and ~3× lower than the bulk Acfer-1 concentration (Pedroni and Begemann, 1994). From this ^{3}He concentration the concentrations of other solar nuclides implanted in the "terrestrial regolith" are derived (Table 1, notes 17 and 18).

The D″ layer is effectively the only source of early-produced ^{129}Xe(I) as well as an important source for ^{136}Xe(Pu). A high ^{129}Xe(I)/^{136}Xe(Pu) ratio seen in some mantle derived samples (e.g., Caffee et al., 1999) constrains the early formation of the layer (see Section 2.1). The model D″ ^{129}Xe(I)/^{136}Xe(U) ratio is rather high (Table 2). Regarding radiogenic over primordial Xe isotope ratios, a value of ^{129}Xe(I)/^{130}Xe$_{DDP}$ ~1000 is inferred from modelling if a solar-like implanted component is considered as the only source of non-radiogenic rare gases in D″. This is in contrast with the analyses of CO_2 gas xenon, in which ^{129}Xe(I)/^{130}Xe ~ 12 (Tolstikhin and O'Nions, 1996). A contribution of a heavy-rare-gas-enriched Q component (Table 1; see Section 5) allows to resolve this contradiction and thus to obtain a more general solution, which now does not require degassing of Q rare gases from a "terrestrial" chondrite. The concentration of Q-gases needed for the reference solution (Table 2) appears to be quite reasonable: it is by a factor of ~ 10^{-3} and ~0.2 lower than those observed in C1 and E chondrites, respectively (Pepin, 1992; Busemann et al., 2000; see Section 5). The mixing proportion Xe_Q/Xe_{SIN}=340, and Q-rare gases contribute ~0.4 of ^{36}Ar to the inventory of this nuclide in D″.

The flux from D″ into the mantle, the mantle degassing flux, and the recycling of atmospheric Xe and Ar were adjusted to obtain model He, Ar and Xe isotope compositions and a ^{3}He-concentration (Table 2) that are similar to the values accepted for the MORB-source mantle. Atmosphere recycling into the mantle is essential: without it, the ^{40}Ar/^{36}Ar derived for the mantle could be as high as ~300,000. The recycling was treated as a flux proportional to atmospheric abundances, with coefficients 0.001 Ga^{-1} for Ar and 0.004 Ga^{-1} for Xe (see Tolstikhin and Marty, 1998; Ballentine and Barfod, 2000 for a detailed discussion of the rare gas recycling-contamination problem). The amount of solar-particle-implanted material in the flux from D″ into the mantle required for a fit is less than 0.05% of the Earth's mass over geological time. A prediction (which also followed from the model of Tolstikhin and Marty, 1998) is that very primitive He and Ne may be found in plume-derived sample, in which a D″-derived solar-like component prevails over radiogenic mantle rare gases.

As mentioned above the crust is not an important reservoir for the terrestrial inventory of radiogenic rare gases. Setting the value of the degassing coefficient $L_{COC,ATM}$ to 0.5 Gyr^{-1} yields a mean ^{40}Ar–^{40}K age for the continental crust that is by ~30% younger that

the Sm–Nd age, 2.2 Gyr. Then the total present-day amount of $^{40}Ar^*$ in the partially degassed crust is ~6% of its total terrestrial inventory. The crustal and mantle concentrations of U and other radioactive elements (Table 2) are in reasonable agreement with available estimates (Weaver and Tarney, 1984; Rudnick and Fountain, 1995; Kramers and Tolstikhin, 1997).

7.3.2. Sm–Nd, Lu–Hf and Rb–Sr isotope systematics

The reference solution for our three-silicate-reservoirs whole-mantle-convective model can be readily derived using fractionation parameters equal or very similar to those derived by other authors. Apart from the formation scenario for D″ (Section 3), the model does not require novel or unusual/unreasonable parameters but uses those already used, discussed and widely accepted, in full accord with Ockham's razor principle.

According to Section 7.3, the rate of crustal growth, the age distribution and mass fluxes into and from the crust are exactly the same as those constrained by Th–U–Pb systematics, which are most sensitive to these parameters (Kramers and Tolstikhin, 1997). A similar crustal growth curve was derived by Jacobsen (1988) and Azbel and Tolstikhin (1988). Other parameters, which govern the distribution of the elements of interest among the three reservoirs, are the melt fractions in the mantle and subduction fractionation zones and the respective partition coefficients.

The mean fraction of liquid silicates in the mantle fractionation zone (mf) during accretion, 0.3, is constrained by modeling of siderophile element partitioning into the metal phase (Section 7.1, see also Kramers and Tolstikhin, 1997; Kramers, 1998). Afterwards this fraction smoothly decreases to the present-day value, ~0.1, derived from the models of mantle melt generation at ridges (e.g., McKenzie and O'Nions, 1991). The melt fraction in the subduction fractionation zone (sf) appears to be a more complicated parameter, which varies substantially, from ~0.01 to ~0.25, the enhanced values 0.1–0.25 being more common for modern arc magmatism (Plank and Langmuir, 1988; McKenzie and O'Nions, 1991). These enhanced melt fractions preclude sufficient fractionation and enrichment of respective melts with highly incompatible elements. This is illustrated by the Rb/Sr ratio in modern subduction-related basalts, ~0.02, by a factor of ~5 below the mean crustal value, whereas high Rb/Sr ratios are observed in ancient crustal igneous rocks. It has been suggested that not only the melt fractions, but also the sources of crust-feeding melts have changed in space and time (e.g., Ellam and Hawkesworth, 1988, and references therein). Investigation of specific mechanisms of continental crust formation in different geological epochs is beyond the frame of this contribution. A simplified approach, i.e., using a small and constant melt fraction in the subduction fractionation zone, was exploited in the layered mantle+crust evolutionary models developed by different authors. Rather similar values of this parameter were derived: 0.005 (Jacobsen and Wasserburg, 1979), 0.01 (Albarède, 1998), 0.015 (Azbel and Tolstikhin, 1988; Kramers and Tolstikhin, 1997; Nägler and Kramers, 1998). We varied the sf melt fraction until the crustal budget of the most incompatible trace elements, U, Th, Rb, was satisfied; a value of ~0.01, very similar to those listed above, was derived (see notes to Table 2).

The REE mineral/melt bulk partition coefficients are reasonably well constrained for mantle mineralogy, as follows from compilations by Jacobsen and Wasserburg (1979), McKenzie and O'Nions (1991) and Nägler and Kramers (1998). Using the solid/melt partition coefficients from these sources, we derive $D(\mathrm{Sm})=0.065$ and $D(\mathrm{Nd})=0.03$ for a mantle peridotite residue with 3% garnet. Using these coefficients for fractionation processes occurring in both mf and sf domains gives a good agreement between calculated and observed abundances of the species of interest in the accessible reservoirs, the mantle and the continental crust (Table 3 and Fig. 1). Because D″ largely consists of fractionated material that was separated from the bulk silicate earth very early, its time-integrated isotopic effect on the mantle is large, of the order of $\varepsilon(\mathrm{Nd}) \approx +5$. Continuous extraction of the continental crust over time leads to a further $\varepsilon(\mathrm{Nd}) \approx +4$ for the mantle, leading to a present day total $\varepsilon(\mathrm{Nd}) \approx +9$ (Fig. 3; see Section 6.2).

The bulk partition coefficient for Hf is, like those for Sm and Nd, considered identical in both mantle fractionation domains mf and sf (Fig. 2b). It is adjusted to produce a crustal Hf/Nd ratio of 0.18, which is intermediate between the upper and lower estimates for the crust (0.19 and 0.17, respectively, e.g. Rudnick and Fountain, 1995). The value is $D(\mathrm{Hf})=0.0385$. The partition coefficient for Lu in the mantle fractionation zone mf, $D(\mathrm{Lu,mf})=0.190$, is adjusted to obtain a somewhat Lu-enriched mantle, so that the mixing line between mantle and crustal end-members approaches the regression of the observed terrestrial Hf–Nd array in Fig. 1. This enhanced value leads to relatively low Lu/Hf ratios and ultimately low $\varepsilon(\mathrm{Hf})$ values in D″ (Table 3, Fig. 1). If true, this could reflect deep partial mantle melting (in the presence of garnet) early in the earth history, when D″ was formed. The solution it provides

to the Hf–Nd isotope problem discussed in Section 2.4 is illustrated in Fig. 1: The chondritic Nd and Hf isotope compositions are enclosed in the triangle defined by D″ and the crust–mantle array.

The bulk partition coefficients for Sm, Nd, Lu and Hf listed above can be independently derived for a melt equilibrated with mantle peridotite consisting of Ol=67%, Opx=20%, Cpx=10%, and Garnet=3% applying the mineral partition coefficients from McKenzie and O'Nions (1991). A similar abundance of garnet in a mantle mineral assemblage (a few percent) was derived by Blichert-Toft and Arndt (1999) in order to explain the enhanced initial $^{176}Hf/^{177}Hf$ ratios in ancient komatiites.

The subduction-fractionation bulk partition coefficient for Lu, 0.145, fits the mantle and crustal end members, so that the mean ε(Hf) values approach the regression line of the terrestrial Hf–Nd array (Fig. 1).

The segregation of D″ very early in Earth history results in an early manifestation of mantle depletion in its model $\varepsilon_{Nd}(T)$ and $\varepsilon_{Hf}(T)$ values, even if early continental crust growth was sparse, as suggested by Th–U–Pb modeling. This is in accordance with observed high initial ε(Nd) values in some ancient rocks (see Fig. 3).

Rb and Sr isotope abundances in the two accessible reservoirs, mantle and crust (Table 3), are in overall agreement with observational data and results derived from other models (Section 6.2). Thus, Jacobsen (1988) inferred from a layered mantle model Sr=15 ppm and Rb/Sr=0.022 for the MORB-source mantle. Recently Workman and Hart (2005) have suggested a much lower Rb/Sr=0.0065. The reason for the difference is that in the latter model a late start of mantle depletion is assumed (at 3 Ga), based on the concept of gradual crustal growth. Further, Workman and Hart (2005) assume depletion of a relatively small portion of the mantle only. Our reference solution ratio, 0.015, is intermediate between the two models. Further, a low Sr for the mantle was obtained from Sr–Ce correlation in MORB samples and Ce concentration derived from mantle melting models (Workman and Hart, 2005). However in other investigations of mantle melting (e.g., McKenzie and O'Nions, 1991) ~1.5 higher Ce (and Sr) concentrations for the depleted mantle are adopted, closer to our estimate.

Sr concentration and Rb/Sr ratio in the bulk continental crust shown in Table 3 for our reference solution are close to the values of Rudnick and Fountain (1995), Sr=325 ppm, and Taylor and McLennan (1985), Rb/Sr=0.12, respectively. However, for Rb–Sr systematics models with discrete lower and upper crustal reservoirs are much more realistic because of preferential Rb migration into the upper crust (e.g., Rudnick and Fountain, 1995). Our reference solution is thus most usefully compared with parameters inferred for an average crust from two-crustal reservoir models: e.g. Sr=410 ppm, Rb/Sr=0.09, and $^{87}Sr/^{86}Sr=0.7090$ (Azbel and Tolstikhin, 1988). The values in Table 3 do not differ greatly from these.

Summarizing, the reference solution shows that a D″ layer as assumed in our model enables to resolve terrestrial paradoxes both of solar and radiogenic noble gases, and of the inventory of incompatible elements. As it is formed from slightly fractionated (enriched) matter and was isolated early, it acts as a second enriched reservoir (in addition to the continental crust) to balance a depleted whole mantle in terms of both incompatible element concentrations and Sm–Nd, Lu–Hf and Rb–Sr isotopic systematics, within the framework of a chondritic Earth model.

8. Summary and conclusions

A D″ layer could have formed in the late stages of the Earth's accretion by subduction of basaltic/komatiitic crust loaded with chondritic regolith (as proposed by Tolstikhin and Hofmann, 2005). The subducted material (containing metal as a major constituent of the regolith and therefore intrinsically more dense than the silicate mantle) could have accumulated at the base of the mantle above the core and stabilized there (as proposed by e.g., Samuel et al., 2003, and Mao et al., 2004). This scenario has important geochemical consequences and enables to reconcile mass balances with whole mantle convection in the framework of a chondritic Earth model.

Our modeling shows that D″ could be an important reservoir containing ~20% of the terrestrial amount of incompatible trace elements. These include heat-generating U, Th and K and therefore a significant portion of radiogenic heat is generated at the base of the silicate mantle, stimulating mantle convection and increasing the heat flow from the depleted mantle.

Because of its early formation and efficient isolation, the D″ layer is the major store for solar, planetary (Q) and early-generated radiogenic rare gas isotopes. Fluxes of mass and/or species from the D″ layer into the convecting mantle and mixing of D″-derived species with the radiogenic components generated in the mantle can explain all observed rare gas isotope patterns, from almost solar in some plume-related samples to those typical of MORB. A small amount of solar-particle-implanted material, less than 0.05% of the Earth's mass,

is enough to maintain the mantle rare gas flow throughout geological history.

The model predicts an extremely high degree of mantle degassing constrained by a low $^{136}Xe(Pu)/^{136}Xe(Pu,U)$ ratio, <0.3, in mantle xenon, especially taken into account that the major portion of $^{136}Xe(Pu)$ is transferred into the mantle from the D″ layer, and the intrinsic mantle ratio (which would have been in the degassed mantle without flux from D″ and from the atmosphere) should be much less than the observed value.

For degassing to reach the levels required by the model, the mantle fractionation rate in the Hadean, and corresponding flux of liquid silicates, should be 2 to 3 orders of magnitude greater than their present day values. With the exception of helium and (in some cases) neon, the heavier non-radiogenic mantle rare gas species are mainly recycled atmospheric components.

Although the Sm/Nd and Lu/Hf fractionation of D″ relative to the BSE is weak, its early isolation causes a substantial isotopic time-integrated effect and thus allows the signatures of ^{147}Sm–^{143}Nd and ^{176}Lu–^{176}Hf in the mantle and crustal reservoirs to be reconciled.

Still much work is needed to verify the proposed origin, history and significance of D″ as an important geochemical reservoir, including modeling of terrestrial regolith accumulation on the surface of an early basaltic crust, its subduction and stabilization at the base of a convecting mantle. The search for such deep ancient reservoir(s) through new isotopic tracers (such as ^{182}W and ^{142}Nd) and noble-metal isotope systematics (e.g., Pt/Os and Re/Os, Brandon et al., 2003) is important. We have merely demonstrated that a D mass (2.3×10^{26} g) in agreement with seismic observations, and a 1/4 proportion of regolithic material required to stabilize it, are adequate to obtain fits to geochemical data in an Earth model with whole mantle convection.

Acknowledgements

Igor Tolstikhin thanks the University of Bern, Switzerland, and Max-Plank Society, the Max-Plank Institute for Chemistry, Mainz, Germany, for the great opportunity to use their facilities during work on this contribution. Programs developed and modified by Dr. Vladimir Asming were used for geochemical modeling of the proposed scenario. We thank Andreas Stracke for giving us his compilation of MORB and PLUME isotopic data and Margarit Vetrin for help with preparing of the Figures. Two constructive reviews by Dr. Conny Class and an anonymous referee were extremely useful for improvements of the manuscript. **[SG]**

References

Albarède, F., 1998. Time-dependent models of U–Th–He and K–Ar evolution and the layering of mantle convection. Chem. Geol. 145 (3–4), 413–429.

Allegre, C.J., 1997. Limitation on the mass exchange between the upper and lower mantle: the evolving convection regime of the Earth. Earth Planet. Sci. Lett. 150 (1–2), 1–6.

Allegre, C.J., Dupre, B., Negrel, P., Gaillardet, J., 1996. Sr–Nd–Pb isotope systematics in Amazon and Congo River systems: constraints about erosion processes. Chem. Geol. 131 (1–4), 93–112.

Anders, E., Grevesse, N., 1989. Abundances of the elements: meteoritic and solar. Geochim. Cosmochim. Acta 53 (1), 197–214.

Angor, C.B., Canup, R.M., Levison, H., 1999. On the character and consequences of large impacts in the late stage of terrestrial planet formation. Icarus 142, 219–237.

Azbel, I.Y., Tolstikhin, I.N., 1988. Radiogenic Isotopes and the Evolution of the Earth's Mantle, Crust and Atmosphere. Kola Sci. Center Pub, Apatity. 140 pp.

Azbel, I.Y., Tolstikhin, I.N., 1990. Geodynamics, magmatism, and degassing of the Earth. Geochim. Cosmochim. Acta 54, 139–154.

Azbel, I.Y., Tolstikhin, I.N., 1993. Accretion and early degassing of the Earth: constraints from Pu–U–I–Xe isotopic systematic. Meteoritics 28, 609–621.

Azbel, I.Y., Tolstikhin, I.N., Kramers, J.D., Pechernikova, G.V., Vitiazev, A.V., 1993. Core growth and siderophile element depletion of the mantle during homogeneous Earth accretion. Geochim. Cosmochim. Acta 57 (12), 2889–2998.

Ballentine, C.J., Barfod, D.N., 2000. The origin of air-like noble gases in MORB and OIB. Earth Planet. Sci. Lett. 180 (1–2), 39–48.

Benkert, J.-P., Baur, H., Signer, P., Wieler, R., 1993. He, Ne, and Ar from the solar wind and solar energetic particles in lunar ilmenites and pyroxenes. J. Geophys. Res. 98 (E7), 13147–13162.

Blichert-Toft, J., Albarède, F., 1997. The Lu–Hf isotope geochemistry of chondrites and the evolution of the mantle–crust system. Earth Planet. Sci. Lett. 148 (1–2), 243–258.

Blichert-Toft, J., Arndt, N.T., 1999. Hf isotope compositions of komatiites. Earth Planet. Sci. Lett. 171 (3), 439–451.

Boyet, M., Carlson, R.W., 2005. ^{142}Nd evidence for Early (>4.53 Ga) global differentiation of the silicate earth. Science 309 (5734), 576–581.

Brandon, A.D., et al., 2003. 186Os–187Os systematics of Gorgona Island komatiites: implications for very early growth of the inner core. Earth Planet. Sci. Lett. 206, 411–426.

Bunge, H.P., et al., 1998. Time scales and heterogeneous structure in geodynamic earth models. Science 280 (5360), 91–95.

Busemann, H., Baur, H., Wieler, R., 2000. Primordial noble gas in "phase Q" in carbonaceous and ordinary chondrites studied by closed-system stepped etching. Meteorit. Planet. Sci. 35, 949–973.

Busemann, H., Baur, H., Wieler, R., 2003. Solar noble gases in enstatite chondrites and implications for the formation of the terrestrial planets, Lunar Planet. Sci. Conf. 34th, Lunar Planet Institute, Houston, pp. abstract #1665, CD-ROM.

Butler, W.A., Jeffery, P.M., Reynolds, J.H., Wasserburg, G.J., 1963. Isotopic variations in terrestrial gases. Geophys. Res. 68, 3283–3291.

Caffee, M.W., et al., 1999. Primordial noble gases from Earth's mantle: identification of a primitive volatile component. Science 285 (5436), 2115–2118.

Carlson, R.W., Lugmair, G.W., 2000. Timescales of planetesimal formation and differentiation based on extinct and extant radio-isotopes. In: Canup, R.M., Righter, K. (Eds.), Origin of the Earth and Moon. The University of Arizona Press, pp. 25–44.

Chambers, J.E., Wetherill, G.J., 2001. Planets in the asteroid belt. Meteorit. Planet. Sci. 36, 381–399.

Chase, C.G., Patchett, P.J., 1988. Stored mafic/ultramafic crust and early Archean mantle depletion. Earth Planet. Sci. Lett. 91 (1/2), 66–72.

Chauvel, C., Blichert-Toft, J., 2001. A hafnium isotope and trace element perspective on melting of the depleted mantle. Earth Planet. Sci. Lett. 190 (3–4), 137–151.

Christensen, U., 1995. Effects of phase-transitions on mantle convection. Annu. Rev. Earth Planet. Sci. 23, 65–87.

Christensen, U.R., Hofmann, A.W., 1994. Segregation of subducted oceanic-crust in the convecting mantle. J. Geophys. Res.-Solid Earth 99 (B10), 19867–19884.

Class, C., Goldstein, S., 2005. Evolution of helium isotopes in the Earth's mantle. Nature 436, 1107–1112.

Clayton, R.N., 2003. Oxygen isotopes in the solar system. Space Sci. Rev. 106, 19–32.

Crisp, J.A., 1984. Rates of magma emplacement and volcanic output. J. Volcanol. Geotherm. Res. 20, 177–211.

DePaolo, D.J., 1980. Crustal growth and mantle evolution: inferences from models of element transport and Nd and Sr isotopes. Geochim. Cosmochim. Acta 44, 1185–1196.

Deruelle, B., Dreibus, G., Jambon, A., 1992. Iodine abundances in oceanic basalts: implications for Earth dynamics. Earth Planet. Sci. Lett. 108, 217–227.

Dixon, E.T., 2003. Interpretation of helium and neon isotopic heterogeneity in Icelandic basalts. Earth Planet. Sci. Lett. 206, 83–99.

Dixon, E.T., Honda, M., McDougall, I., Campbell, I.H., Sigurdsson, I., 2000. Preservation of hear-solar neon isotopic ratios in Icelandic basalts. Earth Planet. Sci. Lett. 180 (3–4), 309–324.

Downes, H., Shaw, A., Williamson, B.J., Thirlwall, M.F., 1997. Sr, Nd and Pb isotopic evidence for the lower crustal origin of Hercynian granodiorites and monzogranites Massif Central, France. Chem. Geol. 136, 99–122.

Ellam, R.M., Hawkesworth, C.J., 1988. Is average crust generated at subduction zones? Geology 16, 314–317.

Goldstein, S.J., Jacobsen, S.B., 1988. Nd and Sr isotopic systematics of river water suspended material: implications for crustal evolution. Earth Planet Sci. Lett. 87, 249–265.

Goldstein, S.L., ONions, R.K., Hamilton, P.J., 1984. A Sm–Nd isotopic study of atmospheric dusts and particulates from major river systems. Earth Planet. Sci. Lett. 70, 221–236.

Grand, S.P., 1994. Mantle shear structure beneath the America and surrounding oceans. J. Geophys. Res.-Solid Earth 99 (B6), 11591–11621.

Harper Jr., C.L., Jacobsen, S.B., 1996. Noble gases and Earth's accretion. Science 273, 1814–1818.

Honda, M., McDougall, I., Patterson, D.B., Doulgeris, A., Clague, D.A., 1993. Noble-gases in submarine pillow basalt glasses from Loihi and Kilauea, Hawaii—a solar component in the earth. Geochim. Cosmochim. Acta 57 (4), 859–874.

Hofmann, A.W., 1988. Chemical differentiation of the Earth: the relationship between mantle, continental crust, and oceanic crust. Earth Planet Sci. Lett. 90, 297–314.

Hudson, G.B., Hohenberg, C.M., Kennedy, B.M., Podosek, F.A., 1982. ^{244}Pu in the early solar system. Lunar and Planetary Science XIII, pp. 346–347.

Ito, E., White, W.M., Gopel, C., 1987. The O, Sr, Nd and Pb isotope geochemistry of MORB. Chem. Geol. 62, 157–176.

Jacobsen, S.B., 1988. Isotopic constraints on crustal growth and recycling. Earth Planet. Sci. Lett. 90, 315–329.

Jacobsen, S.B., Wasserburg, G.J., 1979. The mean age of mantle and crustal reservoirs. J. Geophys. Res. 84, 7411–7427.

Jacobsen, S.B., Wasserburg, G.J., 1980a. Sm–Nd isotopic evolution of chondrites. Earth Planet. Sci. Lett. 50, 139–155.

Jacobsen, S.B., Wasserburg, G.J., 1980b. A two-reservoir recycling model for mantle–crust evolution. Proc. Natl. Acad. Sci. U. S. A. 77, 6298–6302.

Jacobsen, S.B., Quick, J.E., Wasserburg, G.J., 1984. A Nd And Sm isotopic study of the trinity peridotite; implications for mantle evolution. Earth Planet. Sci. Lett. 68, 361–378.

Jochum, K.P., Hofmann, A.W., Ito, E., Seufert, H.M., White, W.M., 1983. K, U and Th in mid-ocean ridge basalt glasses and heat production K/U and K/Rb in the mantle. Nature 306 (5942), 431–436.

Karato, S., Murthy, V.R., 1997. Core formation and chemical equilibrium in the Earth: 1. Physical considerations. Phys. Earth Planet. Inter. 100 (1–4), 61–79.

Kellogg, L.H., 1997. Growing the Earth's D″ layer: effect of density variations at the core–mantle boundary. Geophys. Res. Lett. 24 (22), 2749.

Kellogg, L.H., Wasserburg, G.J., 1990. The role of plumes in mantle helium fluxes. Earth Planet. Sci. Lett. 99, 276–289.

Kellogg, L.H., Hager, B.H., van der Hilst, R.D., 1999. Compositional stratification in the deep mantle. Science 283 (5409), 1881–1884.

Kellogg, J.B., Jacobsen, S.B., O'Connell, R.J., 2002. Modeling the distribution of isotopic ratios in geochemical reservoirs. Earth Planet. Sci. Lett. 204, 183–202.

Kleine, T., Munker, C., Mezger, K., Palme, H., 2002. Rapid accretion and early core formation on asteroids and the terrestrial planets from Hf–W chronometry. Nature 418, 952–955.

Kramers, J.D., 1998. Reconciling siderophile element data in the Earth and Moon, W isotopes and the upper lunar age limit in a simple model of homogeneous accretion. Chem. Geol. 145, 461–478.

Kramers, J.D., 2003. Volatile element abundance patterns and the early liquid water ocean on Earth. Precambrian Res. 126, 379–394.

Kramers, J.D., Tolstikhin, I.N., 1997. Two terrestrial lead isotope paradoxes, forward transport modelling, core formation and the history of the continental crust. Chem. Geol. 139, 75–110.

Kunz, J., Staudacher, T., Allegre, C.J., 1998. Plutonium-fission xenon found in Earth's mantle. Science 280 (5365), 877–880.

Lay, T., Garnero, E.J., Williams, Q., 2004. Partial melting in a thermo-chemical boundary layer at the base of the mantle. Phys. Earth Planet. Inter. 146, 441–467.

Leya, I., Wieler, R., 1999. Nucleogenic production of Ne isotopes in Earth's crust and upper mantle induced by alpha particles from the decay of U and Th. J. Geophys. Res.-Solid Earth 104 (B7), 15439–15450.

Mao, W.L., et al., 2004. Ferromagnesian postperovskite silicates in the DDP layer of the Earth. Proc. Nat. Acad. Sci. 101 (45), 15867–15869.

Matsumoto, T., et al., 2002. Helium in the Archean komatiites revisited: significantly high 3He/4He ratios revealed by fractional crushing gas extraction. Earth Planet. Sci. Lett. 196, 213–225.

McDonough, W.F., Sun, S.-S., 1995. The composition of the Earth. Chem. Geol. 120, 223–253.
McKenzie, D., O'Nions, R.K., 1991. Partial melt distributions from inversion of rare earth element concentrations. J. Petrol. 32 (5), 1021–1091.
Marty, B., Tolstikhin, I.N., 1998. CO_2 fluxes from mid-ocean ridges, arcs and plumes. Chem. Geol. 145 (3–4), 233–248.
Meibom, A., Anderson, D.L., 2003. The statistical upper mantle assemblage. Earth Planet. Sci. Lett. 217, 123–139.
Montelli, R., et al., 2004. Finite-frequency tomography reveals a variety of plumes in the mantle. Science 303, 338–343.
Morbidelli, A., Chambers, J., Lunine, J.I., Petit, J.M., Robert, F., Valsecchi, G.B., Cyr, K.E., 2000. Source regions and timescales for the delivery of water to the Earth. Meteorit. Planet. Sci. 35, 1309–1320.
Moreira, M., Breddam, K., Curtice, J., Kurz, M.D., 2001. Solar neon in the Icelandic mantle; new evidence for an undegassed lower mantle. Earth Planet. Sci. Lett. 185, 15–23.
Muramatsu, Y., Wedepohl, K.H., 1998. The distribution of iodine in the earth's crust. Chem. Geol. 147, 201–216.
Muramatsu, Y., Fehn, U., Yoshida, S., 2001. Recycling of iodine in fore-arc areas: evidence from the iodine brines in Chiba, Japan. Earth Planet. Sci. Lett. 192, 583–593.
Nägler, T.F., Kramers, J.D., 1998. Nd isotopic evolution of the upper mantle during the Precambrian: models, data and the uncertainty of both. Precambrian Res. 91 (3–4), 233–252.
Oganov, A.R., Ono, S., 2004. Theoretical and experimental evidence for a post-perovskite phase of $MgSiO_3$ in Earth's D″. Nature 430, 445–448.
O'Nions, R.K., Oxburgh, E.R., 1983. Heat and helium in the Earth. Nature 306, 429–432.
O'Nions, R.K., Evensen, N.M., Hamilton, P.J., 1979. Geochemical modelling of mantle differentiation and crustal growth. J. Geophys. Res. 84 (11), 6091–6101.
Ozima, M., Podosek, F.A., 2002. Noble Gas Geochemistry. Cambridge Academic Press, Cambridge. 286 pp.
Patchett, P.J., Vervoort, J.D., Soderlund, U., Salters, V.J.M., 2004. Lu–Hf and Sm–Nd isotopic systematics in chondrites and their constraints on the Lu–Hf properties of the Earth. Earth Planet. Sci. Lett. 222, 29–41.
Pedroni, A., Begemann, F., 1994. On unfractionated solar gasses in the H3–6 meteorite Acfer 111. Meteoritics 29, 632–642.
Pepin, R.O., 1992. Origin of noble-gases in the terrestrial planets. Annu. Rev. Earth Planet. Sci. 20, 389–430.
Pierazzo, E., Melosh, H.J., 1999. Hydrocode modeling of Chicxulub as an oblique impact event. Earth Planet. Sci. Lett. 165, 163–176.
Plank, T., Langmuir, C.H., 1988. An evaluation of the global variations in the major element chemistry of arc basalts. Earth Planet. Sci. Lett. 90, 349–370.
Polyak, B.G., Tolstikhin, I.N., 1985. Isotope composition of Earth's helium and the problem of the motive forces of tectogenesis. Chem. Geol. (Isotope Geosci. Sec.) 52, 9–33.
Porcelli, D., Halliday, A.N., 2001. The core as a possible source of mantle helium. Earth Planet. Sci. Lett. 192 (1), 45–56.
Porcelli, D., Wasserburg, G.J., 1995. Mass transfer of helium, neon, argon, and xenon through a steady-state upper mantle. Geochim. Cosmochim. Acta 59, 4921–4937.
Poupeau, G., Kirsten, T., Steinbrunn, F., Storzer, D., 1974. The records of solar wind and solar flares in aubrites. Earth Planet. Sci. Lett. 24, 229–241.
Pritchard, M.E., Stevenson, D.J., 2000. Thermal aspects of a lunar origin by giant impact. In: Canup, R.M., Righter, K. (Eds.), Origin of the Earth and Moon. Univer. Arizona Press, Tucson, USA, pp. 179–196.
Puster, P., Jordan, T.H., 1997. How stratified is mantle convection? J. Geophys. Res.-Solid Earth 102 (B4), 7625–7646.
Righter, K., Drake, M.J., Yaxley, G., 1997. Prediction of Siderophile Element Metal–Silicate Partition Coefficients to 20 Gpa and 2800 °C: The Effects of Pressure.
Rocholl, A., Jochum, K.P., 1993. Th, U and other trace-elements in carbonaceous chondrites: implications for the terrestrial and solar-system Th/U ratios. Earth Planet. Sci. Lett. 117 (1–2), 265–278.
Rudnick, R., Fountain, D.M., 1995. Nature and composition of the continental crust: a lower crustal perspective. Rev. Geophys. 33, 267–309.
Samuel, H., Farnetani, C.G., 2003. Thermochemical convection and helium concentrations in mantle plumes. Earth Planet. Sci. Lett. 207 (39–56).
Samuel, H., Farnetani, C.G., Andrault, D., 2003. Heterogeneous lowermost mantle: compositional constraints and seismological observables. AGU Fall Meeting San Francisco, pp. abstract #T32B-0927.
Schoenberg, R., Kamber, B.S., Collerson, K.D., Eugster, O., 2002. New W-isotope evidence for rapid terrestrial accretion and very early core formation. Geochim. Cosmochim. Acta 66, 3151–3160.
Shukolyukov, A., Lugmair, G.W., 2004. Manganese–chromium isotope systematics of enstatite meteorites. Geochim. Cosmochim. Acta 68 (13), 2875–2888.
Stevenson, D.J., 1990. Fluid dynamic of core formation. In: Newsom, H.E., Jones, J.H. (Eds.), Origin of the Earth. Oxford Univ. Press, New York, pp. 231–249.
Su, Y.J., 2002. Mid-ocean Ridge Basalt Trace Element Systematics: Constraints from Database Management, ICPMS Analyses, Global Data Compilation, and Petrologic Modeling. Columbia University, N.Y.
Swindle, T.D., Podosek, F.A., 1988. Iodine-xenon dating. In: Kerridge, J.F., Matthews, M.S. (Eds.), Meteorites and the Early Solar System. University of Arizona Press, Tucson, pp. 1127–1146.
Taylor, S.R., McLennan, S.M., 1985. The Continental Crust: Its Composition and Evolution. Blackwell Sci. Pub, Oxford. 312 pp.
Tolstikhin, I.N., Hofmann, A.W., 2002. Geochemical importance of the core–mantle transition zone. Eos Trans. AGU 83 (47), F8–F9.
Tolstikhin, I.N., Hofmann, A.W., 2005. Primitive crust on the top of metal magma ocean. Phys. Earth Planet. Inter. 148 (2–4), 109–130.
Tolstikhin, I.N., Marty, B., 1998. The evolution of terrestrial volatiles: a view from helium, neon, argon and nitrogen isotope modelling. Chem. Geol. 147 (1–2), 27–52.
Tolstikhin, I.N., O'Nions, R.K., 1996. Some comments on isotopic structure of terrestrial xenon. Chem. Geol. 129 (3–4), 185–199.
Trieloff, M., Kunz, J., 2005. Isotope systematics of noble gases in the Earth's mantle: possible sources of primordial isotopes and implications for mantle structure. Phys. Earth Planet. Inter. 148, 13–38.
Turner, G., Harrison, T.M., Holland, G., Mojzsis, S.J., Gilmour, J., 2004. Extinct 244Pu in ancient zircons. Science 306, 89–91.
van der Hilst, R.D., Widiyantoro, S., Engdahl, E.R., 1997. Evidence for deep mantle circulation from global tomography. Nature 386 (6625), 578–584.
van Keken, P., Zhong, S., 1999. Mixing in 3D spherical model of present-day mantle convection. Earth Planet. Sci. Lett. 171, 533–547.

van Keken, P.E., Ballentine, C.J., Porcelli, D., 2001. A dynamical investigation of the heat and helium imbalance. Earth Planet. Sci. Lett. 188, 421–434.

van Keken, P.E., Hauri, E.H., Ballentine, C.J., 2002. Mantle mixing: the generation, preservation, and destruction of chemical heterogeneity. Annu. Rev. Earth Planet. Sci. 30, 493–525.

Vervoort, J.D., Patchett, P.J., Blichert-Toft, J., Albarède, F., 1999. Relationships between Lu–Hf and Sm–Nd isotopic systems in the global sedimentary system. Earth Planet. Sci. Lett. 168 (1–2), 79–99.

Vervoort, J.D., et al., 2000. Hf–Nd isotopic evolution of the lower crust. Earth Planet. Sci. Lett. 181 (1–2), 115–129.

Villa, I.M., Renne, P.R., 1998. Decay constants in geochronology. Episodes 20 (1), 1–2.

Wasserburg, G.J., Tera, F., Papanastassiou, D.A., Huneke, J.C., 1977. Isotopic and chemical investigations on Angra dos Reis. Earth Planet Sci.Lett. 35, 294–316.

Wasserburg, G.J., Jacobsen, S.B., DePaolo, D.J., McCulloch, M.T., Wen, T., 1981. Precise determination of Sm/Nd ratios, Sm and Nd isotopic abundances in standard solutions. Geochim. Cosmochim. Acta 45 (12), 2311–2323.

Weaver, B.L., Tarney, J., 1984. Major and trace element composition of the continental lithosphere. Phys. Chem. Earth 15, 39–68.

Wedepohl, K.H., 1995. The composition of the continental crust. Geochim. Cosmochim. Acta 59 (7), 1217–1232.

White, W.M., Schilling, J.-G., 1978. The nature and origin of geochemical variation in mid-Atlantic ridge basalts from the Central North Atlantic. Geochim. Cosmochim. Acta 42, 1501–1516.

Wood, B.E., Muller, H.-R., Zank, G.P., Linsky, J., 2002. Measured mass-loss rates of solar-like stars as a function age and activity. Astrophys. J. 574, 412–425.

Workman, R.K., Hart, S.R., 2005. Major and trace element composition of the depleted MORB mantle (DMM). Earth Planet. Sci. Lett. 231, 53–72.

Yin, Q., Jacobsen, S.B., Yamashita, K., Blichert-Toft, J., Telouk, P., Albarède, F., 2002. A short timescale for terrestrial planet formation from Hf–W chronometry of meteorites. Nature 418, 949–952.